# Path Optimization for Mixed Use of Electric and Fuel Trucks under Multiple Distribution Centers

Xirong Fang, Jian Liu, Lifan Wang

*Abstract*—**In this study, a hybrid vehicle utilization model is proposed to optimize the pickup and delivery problem with time windows under multiple distribution centres (MDC-EFPDPTW) by complementing the advantages of electric and fuel vehicles in response to the high cost and range limitation problems in the development of electric truck technology. A hybrid meta-heuristic algorithm (ALNCO) combining Adaptive Large Neighbourhood Search (ALNS) and Ant Colony Optimisation (ACO) is used to achieve a dynamic balance between local and global search to solve the path problem in the hybrid vehicle mode. Comparative analyses with traditional vehicle modes and mainstream algorithms show that the method has obvious advantages in improving transport efficiency and reducing costs. The study provides a basis for the technological progress and policy formulation of electric trucks and provides new ideas and tools for the green transformation of the transport industry.**

*Index Terms*—**Combinatorial optimization, Electric trucks, Mixed vehicle routing mode, Multiple distribution centers, Green transport transition.**

## I. Introduction

FUELED by global trade and technological advancements, the logistics industry has proliferated, becoming vital to the global supply chain. China's e-commerce boom has significantly boosted the expansion of the express delivery and logistics sectors, where road transport remains dominant, especially for urban and inter-regional deliveries. Despite the industry's contribution to economic growth, transportation costs still account for a large share of logistics expenses, and road transport generates considerable greenhouse gas emissions, posing environmental challenges [1],[2].The logistics industry must enhance efficiency through technological innovation and management optimization to tackle high costs and environmental impacts. Vehicle routing optimization is a widely applied management strategy, with many variants developed for different scenarios. A notable variant for urban distribution is the pick-up and delivery problem with time windows (PDPTW), which focuses on optimizing routes for multiple tasks with time constraints [3], [4].In addition to optimization algorithms, deploying heterogeneous vehicle fleets, including electric and traditional fuel trucks, offers further potential for cost and emissions reductions. Although electric trucks are preferred due to regulatory, financial, and environmental benefits, limitations such as range, charging speed, and infrastructure pose challenges for widespread adoption [5].

As logistics demand grows and urban areas expand, distribution vehicles must cover longer distances, increasing costs. Mixed fleets of electric and fuel trucks may provide an effective solution. Close cooperation between distribution centres allows for more flexible transport planning, optimizing routes and vehicle utilization while integrating electric and fuel trucks [6],[7]. This paper proposes a new model for path optimization in mixed fleets under time constraints, building on existing research in vehicle routing problems. The study explores the synergies and challenges between electric and fuel trucks within a sustainable logistics system, offering insights into their future development.

The main contributions of this research are:

(1) This study proposes a hybrid fleet path optimization model under multiple distribution centers that combine the use of electric and fuel vehicles to solve the time window constraint problem.

(2) The optimization objective function integrates life cycle cost and carbon emission factors, providing a vehicle selection scheme that balances economic efficiency and environmental protection.

(3) A virtual charging station model is introduced, which is designed for electric vehicles, restricts fuel vehicle use, and improves charging infrastructure utilization efficiency.

(4) A hybrid meta-heuristic algorithm (ALNCO) combining ALNS and ACO is proposed. Its performance is compared and analyzed with the exact solver and other mainstream algorithms (e.g., GTS and ALNS).

The paper is organized as follows: Section 2 reviews relevant literature. Section 3 presents the formulation of the mixed fleet vehicle routing problem. Section 4 discusses the ALNCO-based algorithm. Section 5 compares the algorithm's performance, and Section 6 concludes with contributions and future research directions.

## II. Literature Review

In response to the growing demand for logistics and environmental sustainability, vehicle route optimization for pick-up and delivery has attracted significant attention. Existing research primarily focuses on optimizing the delivery routes of traditional fuel trucks and optimizing short-distance delivery routes of electric trucks [8],[9]. Wang et al.[10] and Louati et al.[11] explored optimizing delivery routes for both homogeneous and heterogeneous fleets of fuel vehicles in multi-distribution centres using domain search, column generation, and mixed-integer linear programming methods. Their research highlights significant cost reduction insights in real-world logistics applications, with the potential to improve operational efficiency in various contexts. Polat et al.[12]and Wang et al.[13] took a multi-objective approach, addressing the complex trade-offs between cost, timeliness,

Manuscript received October 20, 2024; revised March 22, 2025.

Xirong Fang is a postgraduate student at the School of Traffic and Transportation, Lanzhou Jiaotong University, Lanzhou 730070, China. (Corresponding author. Phone: +86 18560203018, e-mail: xirongfang@sina.cn).

Jian Liu is a professor at the School of Traffic and Transportation, Lanzhou Jiaotong University, Lanzhou 730070, China. (e-mail: liujian@mail.lzjtu.cn).

Lifan Wang is an engineer at China Railway Xi'an Bureau Group Co., Xi'an 710608, China. (e-mail: xinfenzhenl@sina.com).

and service quality. Their work on synchronous delivery and collection with time windows showcases the importance of balancing multiple factors in logistics optimization. These studies provide critical insights into the flexibility and adaptability required for modern logistics systems, especially as the demand for efficiency and customer satisfaction grows. Focusing on electric trucks, Goeke[14] introduced the Granular Tabu Search algorithm, demonstrating how electric vehicles could improve delivery efficiency and environmental impact, particularly in dense urban settings. Zhang et al.[15] extended this work by incorporating a mutation operator in a multi-objective ant colony optimization algorithm, seeking to minimize operational costs and maximize customer satisfaction. These studies highlight the growing potential for electric trucks in urban logistics, especially as cities increasingly prioritize green transportation initiatives. Phuc et al.[16] and Kececi et al.[17] further explored the practical challenges of optimizing heterogeneous fleets, emphasizing the importance of balancing algorithm complexity with real-world applicability, particularly under strict time windows.

Real-time optimization has become crucial in logistics, particularly with increasing urban congestion and unpredictable road conditions. Kumar et al.[18] proposed a low-complexity real-time traffic information sharing framework that uses roadside units (RSUs) and central servers to dynamically re-plan routes, adapting quickly to road congestion and accidents. Wu et al.[19], on the other hand, introduced an innovative neighbourhood comprehensive learning particle swarm optimization (N-CLPSO) algorithm, which enhances route planning in highly uncertain environments by combining local exploration with global search strategies.

In the Green Vehicle Routing Problems (GVRP) field, researchers have made significant advances in understanding the integration of electric vehicles (EVs) with traditional fuel vehicles in heterogeneous fleet configurations. Sassi et al.[20] and Ying et al.[21] developed models addressing the unique challenges posed by charging infrastructure and carbon emissions. Their findings suggest that the co-existence of electric and traditional vehicles can significantly reduce total transportation costs and carbon footprints. However, limited range and uneven distribution of charging stations remain critical obstacles for large-scale deployment [22]. Zhao et al.[23] built on these models, introducing soft time windows to accommodate charging times, highlighting how strategic planning for charging can reduce overall emissions. Recent research by Celebi[24] and Amiri et al.[25] has also focused on charging infrastructure's role in enhancing electric vehicles' viability in logistics. Celebi[24] emphasized that optimizing charging strategies is essential for expanding electric vehicle usage and ensuring their seamless integration into mixed fleets. Amiri et al.[25] real-world study from Canada underscores the practical benefits of improving charging facilities, showing how infrastructure upgrades can reduce costs and emissions, making electric vehicles more attractive for logistics companies in regions with growing environmental regulations.

Research on vehicle routing in multi-distribution centres has explored how collaborative logistics strategies can drive efficiency and sustainability. Shi et al.[26] emphasized the critical role of collaboration among multiple carriers, showing how shared distribution resources can reduce operational costs and promote environmental sustainability. This is particularly important in the context of modern e-commerce, where fast and efficient delivery is essential for customer satisfaction.Anuar et al.[27] and Zhang et al.[28] extended this work by addressing the dynamic nature of vehicle routing under stochastic conditions, highlighting how advanced optimization techniques, such as approximate dynamic programming and knapsack-based scheduling, can improve decision-making in unpredictable environments. Their findings suggest that flexible, real-time optimization will be key to meeting future logistical challenges. Hou et al.[29] presents an optimization algorithm that aims to combine the fixed cost of the vehicle, the cost of the transport distance, and the cost of the carbon emissions. By selecting an ultra-efficient strategy, the algorithm can achieve a more desirable optimization result under multiple constraints. On the other hand,Wang et al.[30] proposed a hybrid genetic algorithm for optimizing the time-window scheduling and cost-scheduling problems in fresh produce delivery. The algorithm combines the advantages of genetic algorithms and seeks to maximize cost reduction while guaranteeing delivery timelines. Kabadurmus et al.[31] and Ma et al.[32] tackled the challenge of reducing carbon emissions in multi-warehouse vehicle routing problems. By integrating green vehicle routing strategies with heterogeneous fleets, their research demonstrated how mixed-integer linear programming (MILP) models and genetic algorithms (GAs) could optimize both cost and emissions, offering practical solutions for the logistics industry. These findings underscore the importance of adopting environmentally friendly strategies in an industry increasingly held accountable for its environmental impact.

From the reviewed literature, it is clear that further exploration is required in combining fuel-powered and electric trucks for logistics, particularly for pick-up and delivery operations. Most research agrees that electric vehicles are well-suited for short-distance deliveries due to range limitations, while traditional fuel trucks offer more flexibility for longer distances. Coordinated distribution across multiple centres, where electric and fuel trucks operate in tandem, can lead to significant economic and environmental benefits. The relatively low energy costs of electric trucks, combined with the operational flexibility of fuel vehicles, make mixed fleet strategies an attractive option for logistics companies [6].

To address these challenges, this study proposes a novel optimization model, MDC-EFPDPTW, that incorporates real-world operating conditions for mixed fleets, aiming to minimize the total cost of goods transportation. By leveraging an improved domain search algorithm ALNCO, this model offers an innovative solution to the complexities of collaborative distribution from multiple centers. The validity of the model and algorithm proposed in this paper is analyzed using example sets constructed by researchers such as Li et al.[33], providing a theoretical foundation and development suggestions for the joint application of electric and fuel-powered trucks in the logistics and distribution field.

## III. Mathematical Modelling

### A. Problem Description

Fig. 1 illustrates the path planning problem for electric and fuel trucks under multiple distribution centres, comparing transportation modes before and after collaboration. Before collaboration, each distribution centre plans vehicle paths independently, which can result in certain centres handling long-distance tasks, increasing overall transportation distance and energy consumption. Independent planning lacks a global perspective, leading to inefficient resource use, especially in complex multi-centre networks.

In the post-collaboration scenario, vehicle scheduling is optimized through coordination between distribution centres, allowing transport tasks to be distributed more efficiently, reducing the over-concentration of long-distance tasks. The introduction of virtual charging stations ensures that EVs can recharge effectively during transport, improving the feasibility of their task execution.

This forms the basis for the hybrid vehicle path optimization model (MDC-EFPDPTW), which integrates traditional fuel vehicle routing with EV-specific charging constraints and virtual charging stations. The model provides a theoretical framework for optimizing transport efficiency, reducing energy consumption, and lowering carbon emissions.

### *B. Model Construction And Assumptions*

In the $MDC-EFPDPTW$ model proposed in this study, multiple symbols describe the route optimization problem for electric and fuel trucks under a multi-depot distribution scenario. The notations used in the model and their meanings are shown in TABLE I. First, the set of vehicles $K = K_e \cup K_v$ includes all electric and fuel trucks. Each vehicle has unique attributes, including acquisition cost $A^k$, energy consumption per unit distance $\rho^k(x)$, maximum load $U^k$, maximum battery capacity $R^k$, and charging rate $w$. These attributes directly influence the route planning and the calculation of total costs.

In the route planning process, the set of nodes $V\prime$ consists of all depots, customer locations, and charging stations. Since the model focuses on pickup-and-delivery pairs, each delivery task involves transporting goods from a specific pickup point to a corresponding delivery point. Within this framework, routes are categorized into charging and non-charging paths. A non-charging path $(i, j)$ is characterized by a specific distance $d_{ij}$, travel time $t_{ij}$, and the transportation cost for vehicle $k$. The binary variable $x_{ij}^{mk}$ determines whether vehicle $k$ travels on segment $(i, j)$. The model incorporates virtual charging stations to manage electric vehicles' charging requirements efficiently. Unlike actual charging stations, virtual charging stations are designed to simplify the charging paths of electric vehicles and seamlessly integrate them into the pickup-and-delivery pair framework.

Two matched special nodes represent virtual charging stations: the entry node $S\prime$ and the exit node $E\prime$. These nodes represent the "pickup" and "delivery" actions during the charging process. In the route planning process, when an electric vehicle arrives at the entry node $S\prime$, it is akin to "picking up" the required charge, and upon leaving from the exit node $E\prime$, the charging process is completed. The virtual charging stations are defined by the set $F\prime = S\prime \cup E\prime$, where $S\prime = i + g, \ldots, i + \lambda g$ and $E\prime = i + g + f, \ldots, i + \lambda g + f$, with $\lambda$ representing the maximum number of electric vehicles that can charge simultaneously. By matching the entry and exit nodes, virtual charging stations simplify the route and allow multiple electric vehicles to charge simultaneously through replication, thereby avoiding path conflicts and minimizing waiting times.

In route planning, there is no actual distance or time consumption between a virtual charging station's entry and exit nodes; the charging process is treated as a "virtual path." This design aligns with the pickup-and-delivery pair structure of the model, allowing the electric vehicle's charging process to be seamlessly integrated into route planning and preventing the repeated path visits and charging wait issues typically associated with traditional charging station designs.

In this model, each pickup and delivery node $i$ has a fixed service time $S_i$, a time window $[e_i, l_i]$, and a demand $q_i$. The corresponding virtual charging nodes $S\prime$ and $E\prime$ also follow similar service constraints. The service time $S_i$ for a charging station is proportional to the number of electric vehicles needing charging, while the demand $q_i$ for virtual stations is zero. The cost of the path from the entry node $S\prime$ to the exit node $E\prime$ is defined as the charging cost $r_i V_i^{mk}$, where $V_i^{mk}$ represents the amount of charge received by vehicle $k$ at node $i$. This ensures that the model accurately controls the charging costs of electric vehicles and incorporates these costs into the total cost calculation.

To facilitate modelling and ensure the feasibility of the study, the following assumptions are made based on real-world scenarios and relevant literature:

TABLE I
Model parameters and variables

| Variable | Meaning |
|---|---|
| $Z$ | Total cost |
| $k$ | Vehicle |
| $K_e$ | Total electric vehicle |
| $K_v$ | Total fuel vehicles |
| $m$ | Starting point of the distribution centre $m$ |
| $m + g$ | Terminal of the distribution centre $m$ |
| $M$ | All distribution centres, $M = 1, 2, 3, m \in M$ |
| $C$ | Customer point |
| $F'$ | Copy of charging station point |
| $N$ | Customer point and copy of charging station point |
| $N_0$ | Customer point, copy of charging station point, and starting point |
| $N_{n+1}$ | Customer point, copy of charging station point, and endpoint |
| $V'$ | All points |
| $P$ | Set of pick-up points |
| $D$ | Set of delivery points |
| $F'_s$ | Front end of charging station point |
| $F'_E$ | Rear end of charging station point |
| $A$ | Set of edges |
| $A_z$ | Set of non-charging arcs |
| $A_f$ | Set of charging arcs |
| $V_i^{mk}$ | Amount of charge received by vehicle $k$ departing from distribution center $m$ at point $i$ |
| $r$ | Charging cost at the distribution center |
| $r_f$ | Charging cost at the charging station point |
| $w$ | Charging rate |
| $c_k$ | Unit energy cost of vehicle $k$ |
| $\rho^k$ | Unit distance energy consumption of vehicle $k$ |
| $x_{ij}^{mk}$ | Whether vehicle $k$ departing from distribution center $m$ passes through segment $ij$ |
| $y_i^{mk}$ | Battery level of vehicle $k$ departing from distribution center $m$ when leaving point $i$ |
| $q_i$ | Demand at each pick-up and delivery point |
| $R_k$ | Maximum battery capacity of vehicle $k$ |
| $U_k$ | Maximum load capacity of vehicle $k$ |
| $\varepsilon^k$ | Energy carbon intensity of vehicle $k$ |
| $f^k$ | Life cycle cost of vehicle $k$ |
| $o^k$ | Carbon tax for vehicle $k$ |
| $\omega^k$ | Greenhouse gas road emission fee for vehicle $k$ |

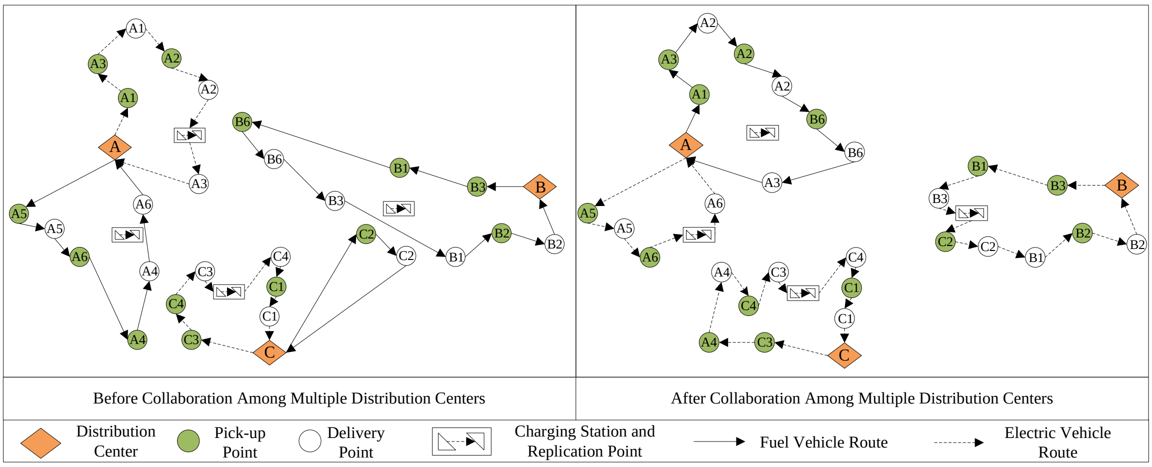
A1
A2
A3
A4
A5
A6
B1
B2
B3
B6
C1
C2
C3
C4
A
B
C
Before Collaboration Among Multiple Distribution Centers
After Collaboration Among Multiple Distribution Centers
Distribution Center
Pick-up Point
Delivery Point
Charging Station and Replication Point
Fuel Vehicle Route
Electric Vehicle Route

Fig. 1. Optimized transportation network: a comparison of multiple distribution centres before and after cooperation

The following assumptions are made in this paper:

(1) The corresponding pick-up point must be located before the delivery point.

(2) The corresponding charging station's front and rear end points must be adjacent, with the front end point positioned first.

(3) The corresponding pick-up and delivery points must be on the same route.

(4) Each delivery vehicle $k$ will start from the distribution centre's starting point and return to the corresponding end point of the distribution centre after completing the delivery task.

(5) Except for the starting and end points of the distribution centre, all other points can only extend outward by one line segment.

To fully address the multi-distribution centre mixed-vehicle scheduling problem, the model introduces four key cost components: charging cost of EVs, fuel cost of fuel vehicles, carbon emission cost, and life cycle cost. First, EV charging costs account for the expenditure at virtual charging stations and distribution centres. This cost constrains EV path selection to avoid scenarios where vehicles run out of power mid-operation, ensuring the optimality of the route. Second, fuel costs are a critical factor for fuel vehicles, reflecting the distance travelled. Despite the growing use of electric vehicles, fuel vehicles remain essential in many scenarios, making it necessary to optimize their operating costs.Third, carbon emission costs are introduced to measure the environmental impact of fuel vehicles and incentivize the use of EVs. By adding this cost, the model aligns with green logistics goals, encouraging a shift towards more sustainable transport solutions. Finally, the life cycle cost ensures that long-term costs, such as vehicle acquisition and maintenance, are appropriately apportioned to path planning. By converting fixed costs into per-unit distance costs, the model avoids large discrepancies between fixed and variable costs. Drawing on the methodology in the literature Li [34], this approach balances both short-term and long-term expenses, ensuring that the economic efficiency of transport operations aligns with the goals of modern green logistics.

Thus, the mathematical model MDC-EFPDPTW can be established as follows:

$$\min Z = Z_1 + Z_2 + Z_3 + Z_4 \tag{1}$$

$$\begin{aligned} Z_1 = &\sum_{m\in M}\sum_{k\in K_e}\sum_{i\in F\prime} r_f V_i^{mk} + \\ &\sum_{m\in M}\sum_{k\in K_e}\sum_{j\in N} r\left(\left(R^k - y_{m+g}^k\right) x_{m_j}^k\right) \end{aligned} \tag{2}$$

$$Z_2 = \sum_{\mathrm{m}\in M}\sum_{k\in K_i}\sum_{i\in N_0}\sum_{j\in N_{n+1}} c^k \rho^k d_{ij} x_{ij}^{mk} \tag{3}$$

$$Z_3 = \sum_{k\in K_v}\sum_{m\in M}\sum_{j\in N_{n+1}} \left(\varepsilon^k o^k \rho^k + \omega^k\right) d_{ij} x_{ij}^{mk} \tag{4}$$

$$Z_4 = \sum_{m\in M}\sum_{k\in K}\sum_{i\in N_0}\sum_{j\in N_{n+1}} f^k d_{ij} x_{ij}^{mk} \tag{5}$$

$$\sum_{j\in N} x_{mj}^k = \sum_{i\in N} x_{i,m+g}^k \leq 1, \forall k \in K, m \in M \tag{6}$$

$$\sum_{x_{ij}}^{mk} = 1, \forall i \in N, m \in M, k \in K, \forall j \in N_{n+1} \tag{7}$$

$$\sum x_{m\prime j}^k = 0, m\prime \in M, k \in K, \forall j \in V\prime \tag{8}$$

$$\begin{aligned} &\sum_{j\in V\prime} x_{ij}^k - \sum_{j\in V\prime} x_{j,i+n}^k = 0, \forall i \in P, k \in K, \\ &m \in M \end{aligned} \tag{9}$$

$$\sum x_{ij}^{mk} \leqslant 1, (i, j) \in A_f, k \in K_e, m \in M \tag{10}$$

$$\sum x_{ij}^{mk} = 0, (i, j) \in A_f, k \in K_v, m \in M \tag{11}$$

$$e_i < T_i^{mk} < l_i, \forall i \in N \cup F\prime, k \in K, m \in M \tag{12}$$

$$\begin{aligned} &T_i^{mk} + S_j + t_{ij} - M\left(1 - x_{ij}^{mk}\right) \leqslant T_j^{mk}, \\ &\forall i \in V\prime, \forall j \in V\prime, k \in K, m \in M, i \neq j \end{aligned} \tag{13}$$

$$\begin{aligned} &S_i + T_i^{mk} + t_{i,n+i} \leqslant T_{i+n}^{mk}, \forall i \in P, k \in K, \\ &m \in M \end{aligned} \tag{14}$$

$$\begin{aligned} &S_i + T_i^{mk} + t_{ij} \leqslant T_j^{mk}, \forall (i, j) \in A_f, k \in K_e, \\ &m \in M \end{aligned} \tag{15}$$

$$S_i = V_{ij}^{mk}/w, \forall (i,j) \in A_f, k \in K_e, m \in M \tag{16}$$

$$u_i^{mk} + q_j - M\left(1 - x_{ij}^{mk}\right) \leqslant u_j^{mk}, \forall i \in V', \\ j \in V', k \in K, i \neq j, m \in M \tag{17}$$

$$y_j^{mk} \leq y_i^{mk} - \rho^k d_{ij} x_{ij}^k + R^k\left(1 - x_{ij}^{mk}\right), \\ \forall (i,j) \in A_z, k \in K_e, m \in M \tag{18}$$

$$V_{ij}^{mk} = x_{ij}^{mk}\left(y_j^{mk} - y_i^{mk}\right), \forall (i,j) \in A_f, k \in K_e, \\ m \in M \tag{19}$$

$$y_j^{mk} \leqslant y_i^{mk} + V_{ij}^{mk}, \forall (i,j) \in A_f, k \in K_e, i \neq j, \\ m \in M \tag{20}$$

$$x_{ij}^{mk} = \{0,1\}, \forall i \in V', \forall j \in V', i \neq j, \forall k \in K, \\ m \in M \tag{21}$$

$$R_k \geqslant y_i^{mk} \geq 0, i \in V', \forall k \in K_e, m \in M \tag{22}$$

$$R_k \geqslant V_i^{mk} \geqslant 0, \forall i \in F', \forall k \in K_e, m \in M \tag{23}$$

$$U_k \geqslant u_i^{mk} \geqslant 0, i \in V', m \in M \tag{24}$$

$$d_{ij} \geqslant 0, \forall i \in V', j \in V', i \neq j \tag{25}$$

Equation (1) represents the objective function, which is composed of the electricity cost $Z_1$ for electric trucks, the fuel cost $Z_2$ for fuel trucks, the carbon emission cost $Z_3$, and the entire life cycle cost $Z_4$ for both electric and fuel trucks. Equation (2) calculates the electricity cost for electric trucks, where the first term represents the total cost of charging vehicle $k$ at all charging stations, calculated as the amount of charge required multiplied by the unit charging cost, and the second term represents the cost of fully charging vehicle $k$ at the distribution centre when it departs from centre $m$, ensuring that the vehicle is fully charged for the next delivery, with a charge level of $y_{m+g}^{k}$ upon return. Equation (3) represents the fuel cost for fuel trucks. Equation (4) calculates the carbon emission cost, and Equation (5) represents the life cycle cost for electric and fuel trucks.

Equation (6) ensures that each vehicle starts from the distribution centre's starting point and returns to the corresponding endpoint. Equations (7) and (8) ensure that, apart from the distribution centre's start and end points, each point can only extend one line segment outward, and no line segment can extend from the endpoint. Equation (9) ensures that the exact vehicle transports pick-up and delivery requests on the same route. Equations (10) and (11) limit each virtual charging station to be visited by the same electric truck at most once and prevent visits by fuel trucks. Equations (12) and (13) represent the time window constraints for each point. Equation (14) requires that the front end of a matching pick-up point precedes the front end of a delivery point. Equations (15) and (16) ensure that the front end of a charging arc precedes the rear end of the charging arc. Equation (17) addresses vehicle capacity constraints, and Equations (18) to (20) represent power constraints for electric vehicles. Equation (21) indicates whether vehicle $k$ from distribution centre $m$ passes through line segment $ij$. Equation (22) indicates the battery level of electric vehicle $k$ from distribution centre $m$ at point $i$. Equation (23) represents the amount of charge for electric vehicle $k$ at point $i$. Equation (24) indicates the load of vehicle $k$ at point $i$, and Equation (25) represents the distance of line segment $ij$.

In vehicle path planning, uncertainties such as fluctuating travel times, charging station availability, and variable customer demand add complexity. While these factors are critical, addressing them would significantly increase the model's complexity. Thus, to maintain the solvability and practicality of the model, we focus on deterministic optimization. Future research will address these uncertainties by incorporating stochastic elements into the ALNCO algorithm, enhancing the model robustness and broadening its applicability in practical scenarios.

## IV. Algorithm Design

This study explores a variant of the PDPTW problem (Pickup-Delivery with Time Window problem), which belongs to the category of NP puzzles. In the case of hybrid vehicle configurations, this paper classifies the problem into two categories: fuel-powered trucks that do not need to pass through a charging station and electric trucks that need to pass through a charging station. Therefore, the problem presented in this study is more challenging in terms of complexity than the traditional PDPTW problem. In recent years, metaheuristic algorithms have been widely used to solve PDPTW problems. However, a literature review reveals no research on multi-distribution point PDPTW models for hybrid vehicle configurations. In this study, a combinatorial metaheuristic algorithm (ALNCO) is developed based on the latest literature to find an optimal solution for this problem, which in turn provides a new research perspective in this research area. This chapter first describes how to encode customer points using pickup-delivery strategies, then discusses the initial solution generation method, and finally, elaborates on the design of the ALNCO algorithm, including its key steps, main modules, and algorithmic flow, aiming to efficiently solve the multi-delivery-point PDPTW problem with mixed vehicle configurations.

### A. Pickup-delivery Pairing Strategy

As illustrated in Fig. 2, this study's vehicle routing model ensures that each pair of pick-up and delivery points is processed simultaneously and that charging stations and their replicas are efficiently utilized.

In the model, the numbering begins by assigning collection point numbers, starting from 0, followed by the numbering of pick-up points, delivery points, charging stations, charging station replicas, and distribution centre points. The model includes three main points: customer points (pick-up and delivery), charging stations (and replicas), and distribution centre points. These points are integrated into a list that forms the basis for generating a comprehensive numbering system. The numbering system is subdivided into customer points, charging stations, and distribution centers. Each pair of pick-up and delivery points is assigned a matching identifier number, ensuring that the same vehicle is always served by the same vehicle throughout the routing process. For example, in Fig. 2, the pair of pick-up and delivery points with a matching identifier "A1a" is processed together by a single vehicle. This binding strategy ensures that pick-up and delivery pairs remain intact during each algorithm iteration,

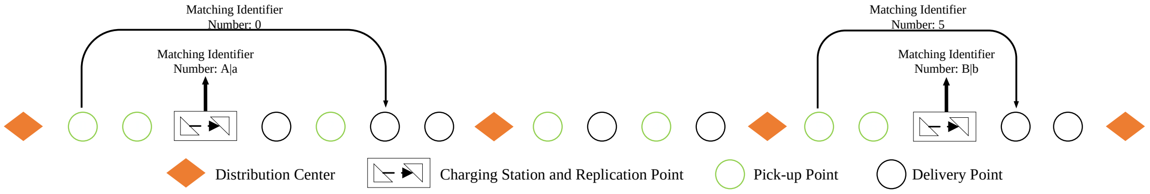

Fig. 2. Example of the composition of the general route number

improving route efficiency. Furthermore, the model defines matching identifier numbers for each charging station's front-end and rear-end points and replicas. This ensures that charging stations' front-end and rear-end points are connected, allowing electric vehicles to utilize the charging infrastructure effectively. In Fig. 2, for instance, charging stations are represented with their respective identifiers, ensuring continuity between the front and rear points. The total driving route for each distribution center is represented by a list of numbered points, where the intervals between distribution centers represent the vehicle's driving path. Odd-numbered routes are assigned to electric vehicles, while even-numbered routes are designated for fuel vehicles. Power constraint checks are applied to electric vehicle routes, and charging stations are inserted to ensure optimal charging infrastructure utilisation.

### B. Initial Solution

The route iteration process begins by generating vehicle routes and ensuring optimal use of charging stations. The initial solution is generated as follows:

Step 1: Assign each pair of pickup and delivery points to the closest distribution center $m$ and assign vehicles $k$ to each center based on the number of tasks at each center.

Step 2: Generate a list of routes $L$ containing distribution center numbers, with odd numbers being electric and even fuel vehicle routes. The list of pickup and delivery points $H$ is sorted according to the distance between the pickup and delivery point and the distribution center $m$ from the nearest to the farthest.

Step 3: Insert each pair of pickup and delivery points from list $H$ into route list $L$ in order, ensuring that the pickup point is before the delivery point. Customer points are inserted according to the distance-first rule.

Step 4: Check the constraints for each request $q$. For fuel vehicles, capacity and time window constraints must be satisfied; power constraints are also checked for electric vehicles. If all constraints are satisfied, continue processing; otherwise, go to Step 5.

Step 5: If the insertion fails due to power constraints, mark the sub-route as secondary and pause further insertion operations. Place the unsatisfied request $q$ at the end of the pickup and delivery point list $H$.

Step 6: Insert a charging station in the secondary sub-route to satisfy the electric vehicle's power requirement. After inserting the charging station, return to Step 4 and recheck all constraints for the route.

### C. ALNCO

In the MDC-EFPDPTW model, the traditional ALNS local search is limited by the delivery and charging constraints, resulting in unstable solution quality. To solve this problem, this paper proposes a dynamic feedback and parallel optimization algorithm (ALNCO) that combines ACO through the parallel optimization and bidirectional feedback mechanism of ALNS and ACO to improve search efficiency and solution quality. The core of the method lies in the parallel optimization and feedback mechanism, where ALNS and ACO share the initial solution, perform optimization, and exchange information separately in order to achieve a close integration of local and global search. The specific process is shown in Algorithm 1:

The algorithm generates an initial solution via a greedy algorithm, which serves as the starting point for both ALNS and ACO.ALNS performs local optimization via node destruction and insertion operations, while ACO guides the ant colony to perform a global search using pheromone and heuristic information. Both are executed in parallel to ensure that the local and global searches are synchronized to optimize the local quality of the solution and extend the search space.In order to enhance the synergy between local and global search, the algorithm introduces a two-way feedback mechanism: the ACO uses pheromone concentration to guide the ALNS's deletion operation, which preferentially removes poor-quality paths and avoids local optimums; and the ALNS adjusts the path selection probability of the ACO through its optimisation experience to enhance the efficiency of the global search.

In the feedback phase, ACO adaptively adjusts the pheromone volatility rate according to the optimization information provided by ALNS to maintain a high concentration of high-quality paths; at the same time, ALNS dynamically adjusts the destruction intensity and balances the breadth and depth of the search. At the end of each iteration, the algorithm compares the optimal solutions of the two and selects the optimal solution as the initial solution of the next round, gradually approaching the global optimal solution and accelerating convergence.

*1) ALNS Operation:* Multiple executions of the ALNS algorithm can be time-consuming, and the quality of the solution is usually sub-optimal due to its wide local search.

**Algorithm 1** ALNCO dynamic feedback and parallel optimization

```
Input: Node list, distance matrix, parameter set
Output: Objective function value
Generate an initial solution, initialize ALNS and ACO parameters, and segment optimization table
Set total iterations $ite3$ and threshold $con3$
Parallel optimization process:
while Current iteration < $ite3$ and optimization improvement > $con3$ do
    # ALNS operations
    for iteration $i$ from 1 to $ite1$ or optimization improvement > $con1$ do
        Perform deletion and insertion operations
        Update the best solution and segment optimization table
        Dynamically adjust the probabilities of each deletion and insertion operation
    end for
    # ACO operations
    for iteration $i$ from 1 to $ite2$ or optimization improvement > $con2$ do
        Ant colony selects paths based on pheromone concentration
        Update the solution and pheromone concentration
    end for
    # Dynamic feedback and interaction
    ACO adjusts path selection probabilities via the segment optimization table
    ALNS pheromone concentration operation updates the pheromone concentration
    Adaptively adjust the ACO pheromone evaporation rate
end while
Output the global best solution
```

In this paper, we increase the local search randomness by parameter tuning and reduce the number of iterations to shorten the running time, improving the running efficiency and maintaining the solution quality.

ALNS consists of an outer and inner loop, with the outer loop controlling the total number of iterations and the inner loop dynamically adjusting the solution space through destruction and repair operations, using the temperature mechanism of simulated annealing (SA) to accept poorer solutions with a certain probability. The weights of the destruction and repair operations are updated based on the forgetting factor $\lambda$, the score $S_w$ and the frequency of use $V_w$, and the operations are selected using a roulette mechanism:

$$R_w^{i+1} = R_w^i \lambda + (1 - \lambda) \frac{S_w^i}{V_w^i} \tag{26}$$

The operation selection probability is:

$$P_{\mathrm{w}}^i = \frac{R_w^i}{\sum_{j \in n} R_j^i} \tag{27}$$

The scoring mechanism classifies the solutions into four categories, giving different scores based on improvement. The simulated annealing acceptance criterion follows the Metropolis rule, where the probability $P$ of accepting a worse solution decreases as the temperature decreases, Eq:

$$P = \exp\left(\frac{C_u^i - C_n^i}{T}\right) \tag{28}$$

The inner loop gradually decreases the temperature, and after reaching the critical temperature, the outer loop is incremented until the termination condition is satisfied.

In order to make the model of this paper applicable to the ALNS algorithm, based on the research of Ropke et al.[4], two insertion operations and four deletion operations are set up: pheromone concentration insertion, marginal cost insertion, Shaw deletion, pheromone concentration deletion, marginal cost deletion and minimum service set deletion.

These operations optimize the quality of the solution and the global search effect through different strategies. Pheromone Concentration Insertion is based on the global pheromone concentration fed back from the ACO and prioritizes the insertion of deleted customer points in path segments with high concentration, where higher pheromone concentration indicates that the path performs better in the ACO's global search, thus improving insertion effectiveness. Marginal cost insertion reduces the overall transportation cost and improves efficiency by calculating the new cost of each insertion location and selecting the location with the smallest increase in cost. Shaw deletion considers several variables: distance, time window, and demand. It starts deleting highly correlated customer points from randomly selected customer point locations to optimize the local solution while improving the diversity of the search. Pheromone concentration deletion prioritizes the removal of path segments with low pheromone concentration in the ACO search, as these paths perform poorly in the global search, and removing them helps the algorithm to jump out of the local optimum and explore better solutions. Marginal cost deletion allows the algorithm to focus on reducing the overall cost and improving the quality of the solution by removing the customer points that contribute the least to the current solution. On the other hand, the minimum service set deletion operation focuses on removing vehicle tasks that serve only a few customers, optimizing the overall transport efficiency by freeing up the resources of these vehicles and reallocating them to more efficient vehicles.

Take the insertion operation as an example: this operation loops through all elements in the solution list, exploring every possible insertion position. The specific process is illustrated in Fig. 3.

First, a contiguous delivery area is identified, beginning at point a and ending at point b, where b represents the first distribution centre encountered to the right of a. Each delivery area is then divided into a fuel vehicle operation area and an electric vehicle operation area, based on the type of vehicle in use. Within the designated area, attempts are made to insert the pending pick-up and delivery points at appropriate locations, determined by the type of vehicle operating in that area. For electric vehicle operation areas, charging stations are inserted at optimal locations to enhance the efficiency of charging station utilization, taking into account the charging requirements of the electric vehicles.

In the charging station insertion operation, the sequence in which vehicle $k$ passes each customer point has already

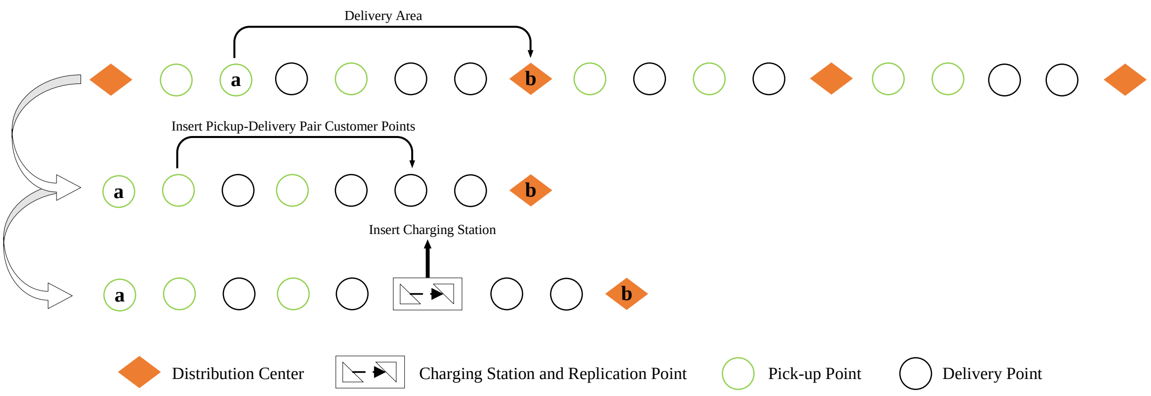

Fig. 3. Insert operation process

been determined, ensuring that all constraints are satisfied. The goal now is to insert charging stations efficiently. This process is mathematically modelled as follows:

$$\min_{k} = \sum_{i \in F} r_i V_i^{mk} + r\left(R^k - y_{m+g}^k\right) \tag{29}$$

$$0 \leqslant \sum_{i \in F} |i| \leqslant \left| \frac{\sum^{ij} D^k}{R^k} \right|, (i, j) \in M \tag{30}$$

$$\begin{cases} D_{ij}^f \leqslant \frac{\sum_{i \in M} D_{ij} \rho^k}{|F|}, if \frac{\sum_{ij \in M} D_{ij} \rho^k}{|F|} \geqslant \frac{r_f}{r} \min D_{ij}, \\ f \in A_f, (i, j) \in M \\ D_{ij}^f \leqslant \frac{r_f}{r} \min D_{ij}, if \frac{r_f}{r} \min D_{ij} \geqslant \frac{\sum_{i \in M} D_{ij} \rho^k}{|F|}, \\ f \in A_f, (i, j) \in M \end{cases} \tag{31}$$

Equations (29), (30), and (31), along with equations (12) to (20), form the model for the charging station insertion operation. Equation (29) addresses vehicle $k$, which departs from the distribution centre $m$ and visits a series of designated customer points, with charging stations inserted at optimal locations to minimize total cost. Equation (30) determines the maximum number of charging stations that can be inserted by calculating the total distance travelled by the vehicle without visiting charging stations, taking into account the vehicle's power consumption per kilometre and the maximum battery capacity. Equation (31) constrains the insertion location of the charging station to ensure that the selected station is both economically and operationally efficient. This involves calculating the average distance for each route from customer point $i$ to a charging station and then from the charging station to customer point $j$, as well as determining the minimum distance for all possible routes from customer point $i$ to a charging station, and then from the charging station to customer point $j$. By comparing the maximum distance values obtained from these calculations, less optimal charging stations can be excluded from consideration, reducing computational time and improving the overall efficiency of the process.

To further improve the ALNS performance, this paper introduces a path segment optimization table to record the performance of each path segment in multiple iterations and guide the selection of subsequent operations with historical information. The path segment score is dynamically adjusted according to its impact on the objective function, and the path segments with good performance will be prioritized for subsequent operations. In each ALNS execution, the initial score of a path segment is $h_{ij}$, if the operation improves the objective function, the score increases; otherwise the score decreases. The score update formula is:

$$h_{ij}^{\text{new}} = h_{ij}^{\text{old}} \times \lambda + (1 - \lambda) \times R_{ij} \tag{32}$$

Where $\lambda$ is the forgetting factor and $R_{ij}$ denotes the performance of the path segment in the current iteration. Path segments with good historical performance will be preferred through this dynamic scoring mechanism in subsequent operations.

*2) ACO Operation:* Based on the MDC-EFPDPTW model, this paper improves the Ant Colony Optimisation (ACO) algorithm and introduces a path segment optimization table $h_{ij}(s)$ to improve the algorithm performance. The table records the performance of path segments over multiple iterations and guides the ants in selecting the optimal path.

Equations (33) and (34) show that the pheromone concentration $\Delta\tau_{ij}$ released by ant colony $F$ between path segments $ij$ in each iteration is obtained by accumulating pheromone released by individual ants:

$$\Delta\tau_{\text{ij}}^{f} = \frac{Q}{Cf} h_{ij}(s), f \in F \tag{33}$$

$$\Delta\tau_{ij} = \sum_{f \in F} \Delta\tau_{ij}^{f} \tag{34}$$

Where $h_{ij}(s)$ denotes the performance of the path segment in historical iterations, the better the performance, the higher the value of $h_{ij}(s)$. $Q$ is the total cost of the worst performing ant in the colony, and $C_f$ is the total cost of ant $f$. If the path segment $ij$ is not passed by ant $f$, then $\Delta\tau_{ij}^{f} = 0$.

The rule for generating a feasible ant set $N$ is to generate a feasible set through two rounds of filtering as ants move from point $i$ to point $j$. The first round extracts the set $N$++ of ants that satisfy the criteria from $i$ to $j$ from the original set $F$, with $j$ denoting the points that have not yet been visited. The second round of filtering checks the constraints and removes the ants that do not satisfy them to obtain the final feasible set $N$.

Equation (35) describes the update of the global pheromone concentration:

$$\tau_{ij}(s+1) = \rho\tau_{ij}(s) + \Delta\tau_{ij} \tag{35}$$

Here, $\tau_{ij}(s+1)$ is the pheromone concentration of the path segment $ij$ after the $s+1$th iteration, which contains the remaining pheromone after volatilization and the added pheromone concentration. When $s = 0$, $\tau_{ij}(s) = 0$.

The probability of an ant moving from point $i$ to point $j$ in each iteration is given by equation (36):

$$p_{ij}^{f} = \frac{\tau_{ij}^{\alpha}(s)\eta_{ij}^{\beta}(s)h_{ij}^{\gamma}(s)}{\sum_{n\in N^f}\tau_{ij}^{\alpha}(s)\eta_{ij}^{\beta}(s)h_{ij}^{\gamma}(s)}, j \in N^f \tag{36}$$

Where $j \in N^f$ is the accessible point of ant $f$, generated by two rounds of filtering. The first round removes path segments with zero pheromone concentration to obtain the initial set $N^g$; the second round checks the constraints and removes path segments that do not meet the requirements to obtain the final set $N^f$. In the equation, $\tau_{ij}^{\alpha}(s)$ is the pheromone concentration of the ants on the path segment $ij$ in the $s$th iteration, $\eta_{ij}^{\beta}(s)$ is the reciprocal of the distance from the point $i$ to the point $j$, and $h_{ij}^{\gamma}(s)$ is the weights of the optimization table of the path segments to guide the ants to prioritize path segments that have performed well in historical iterations.

*3) Dynamic Feedback And Interaction:* In the ALNCO algorithm, the dynamic feedback and interaction mechanism achieves the collaborative optimization between ALNS and ACO through bidirectional information exchange. The ACO refers to the history strategy table $h_{ij}(s)$ in path selection, while the ALNS dynamically adjusts the local search operation based on the global information fed back by the ACO, thus forming an effective closed-loop feedback process. The history strategy table records the local search performance of the path segments, which affects the pheromone volatility of the ACO and the ALNS operation weights, thus improving the global convergence speed and local search quality.

First, the ACO uses the history strategy table $h_{ij}(s)$ to prioritize well-performing path segments over multiple iterations during path selection. The $h_{ij}(s)$ records the performance of path segments $ij$ over multiple iterations with scores based on ALNS local search feedback. By adjusting the path selection probability, $h_{ij}(s)$ is introduced as an additional weight $\gamma$ into the classical ACO path selection formula, which, together with the pheromone concentration $\tau_{ij}(s)$ and the heuristic information $\eta_{ij}(s)$ determines the priority of the path selection so that the ACO can better incorporate the historical feedback information and prioritize the exploration of efficient paths and avoid ineffective exploration of low-quality paths.

In the ALNS operation, the pheromone concentrations fed back by the ACO guide the deletion and repair operations. For the deletion operation, ALNS decides the priority path segments to be deleted based on the pheromone concentration of the path segments fed back by the ACO. Path segments with lower pheromone concentration usually perform poorly in the global search of the ACO, and prioritizing removing these path segments reduces the duplication of explorations and improves the diversity of local searches. For the repair operation, ALNS prioritizes the repair of path segments with higher pheromone concentration, thus improving the quality of the local solution. With the global information guidance in ACO, ALNS can better retain the well-performing path segments and avoid falling into local optima.

In addition, the volatility of pheromone concentration in ACO is also affected by the history strategy table, which further enhances ACO's global search capability. In each iteration, the pheromone concentration of the path segments not only naturally decays according to the volatility rate $\rho$, but also adaptively adjusts according to the history strategy table $h_{ij}(s)$. For a path segment that performs well in the strategy table, its pheromone volatilization rate decreases, and it is retained for a longer period, attracting more ants to choose that path segment. On the contrary, for poorly performing path segments, the volatilization rate increases, and the pheromone decays rapidly, thus reducing the impact of these path segments in subsequent iterations and avoiding repeated exploration of invalid paths.

The following equation can describe the volatility adjustment mechanism: set the base volatility rate $\rho_0$ and adaptively adjust it according to the value $h_{ij}(s)$ recorded in the historical strategy table. The adjustment formula is:

$$\rho_{ij}(s+1) = \rho_0 - k \times h_{ij}(s) \tag{37}$$

Where $\rho_{ij}(s+1)$ denotes the actual volatility of the path segment $ij$ after the $s+1$th iteration, $\rho_0$ is the default base volatility, $h_{ij}(s)$ is the performance of the path segment in the historical strategy table, and $k$ is the adjustment factor. Through this dynamic adjustment mechanism, the volatility rate $\rho_{ij}(s+1)$ changes adaptively based on the historical performance of the path segment, affecting the pheromone update process.

The updated pheromone equation is:

$$\tau_{ij}(s+1) = \rho_{ij}(s+1)\tau_{ij}(s) + \Delta\tau_{ij}(s) \tag{38}$$

Where $\rho_{ij}(s+1)$ is the dynamically adjusted volatility, $\tau_{ij}(s)$ is the pheromone concentration of the path segment in $s$ iterations, and $\Delta\tau_{ij}(s)$ is the new pheromone released by the ants on the path segment in the current iteration. This adjustment mechanism allows the pheromone of the better-performing path segments to be retained for a more extended period, thus increasing the probability of being selected in the subsequent iterations. In contrast, their pheromone volatilization rate is higher for poorly performing path segments, and their concentration decays rapidly, reducing their impact in the global search. This adaptive adjustment mechanism ensures that the global search capability of the ACO is maximized while reducing the over-exploration of sub-optimal paths.

The dynamic feedback and interaction mechanisms enable ALNS and ACO to form a tightly coupled optimization process.ACO provides feedback on the global perspective of path selection through the history strategy table and adaptively adjusts the volatility to enhance the exploration of high-quality paths.ALNS, on the other hand, guides the deletion and repair operations through pheromone concentration to optimize the local search and avoid the repetitive exploration of low-quality paths, thus improving the overall quality of the solution. Through this two-way feedback mechanism, ALNS and ACO continuously optimize the algorithm parameters in each round of iteration to improve the efficiency and stability of the algorithm and achieve the synergistic optimization effect of global and local search.

## V. Numerical Study

In this chapter, a series of numerical experiments are presented to evaluate the performance and sensitivity of the proposed model solutions. Specifically, Section 3.1 details the design of the benchmark test instances and the configuration of their parameters. Section 3.2 explores the testing process for the models' performance, covering both small and large instances. In Section 3.3, the solutions for small instances, generated using the commercial solver Gurobi, are compared with the algorithm proposed in this study and the GTS algorithm by Goeke[14]. Finally, Section 3.4 focuses on the solutions for large instances, comparing the GTS algorithm by Goeke[14], the algorithm developed in this study, and the ALNS algorithm.

### A. Parameters And Numerical Settings

All experiments in this study were conducted on a computer equipped with an Intel Core i7-3650 processor, with parallel optimization algorithms implemented. The algorithm was developed in Python 3.9, utilizing multi-threading to improve computational efficiency. The test parameters included: max-percentages (controlling the maximum percentage of certain operations during local search), tau (adjusting the threshold for specific adaptive mechanisms in the algorithm), cooling rates (adjusting the cooling rate in the simulated annealing algorithm), reaction-factors (determining whether to accept a new solution during local search), noise factors (introducing randomness to escape local optima and increase solution diversity), $\alpha$ (reflecting the importance of pheromone accumulation in guiding the ant colony search), $\beta$ (reflecting the importance of heuristic information in guiding the ant colony search), and $\rho$ (indicating the level of pheromone retention). The parameter settings were referenced from Ropke et al.[4] and further refined in this study.

The method for solving the parameter settings is referenced from Ropke et al.[4] and has been improved upon in this study. The initial parameter value settings and processing procedures still follow Ropke's method. For each optimal parameter selection, the number of operations for each instance is increased to generate more solutions, and the deviation of each test instance from the known optimal solution is calculated for each run. The parameter value range list is then traversed, and the average and standard deviation deviations for all runs are computed. An upper limit is set for the standard deviation to exclude parameter configurations with small average deviations but exhibit large fluctuations in deviations. The optimal parameter values were finally determined to be: 8% for max-percentages, 0.04 for $\tau$, 0.999 for cooling rates, 0.15 for reaction factors, 0.025 for noise factors, 1 for $\alpha$, 3 for $\beta$, and 0.4 for $\rho$.

The maximum number of iterations is 500, and the iteration is stopped when the optimization margin is less than 0.01 for 30 consecutive accumulations. Suppose the result of an iteration is significantly worse than the current solution. In that case, the optimization has not progressed, the iteration is not counted in the consecutive cumulative number of times, and the subsequent iterations continue until the stopping condition is met or the maximum number of iterations is reached.

The vehicle-related parameters used in this study are consistent with those selected in Amiri[25]. The cost of a pure electric truck is 1.05 million yuan, while the cost of a fuel truck is 875,000 yuan. The energy consumption of an electric truck is 1.75 kWh/km, whereas the energy consumption of a fuel truck is 2.5 times that of an electric truck. The full life cycle cost $f^k$ is derived from the full life cycle cost formula in Li[34]. Since this study focuses on long-distance truck delivery with a limited number of vehicles, and the carbon emission fee is calculated separately, only the tangible costs are considered in the full life cycle cost. Please refer to Li[34]for further details. The $CO_2$ emission factor for fuel vehicles is 3.096 kg/l, based on data from the United Nations Intergovernmental Panel on Climate Change [23]. The carbon tax used in this paper is set at 43 yuan/tonne of $CO_2$ equivalent, as reported by the 2021 International Council on Clean Transportation (ICCT) in their report Comparative Analysis of the Total Cost of Ownership of Heavy-Duty Trucks in China: Pure Electric, Fuel Cell, and Diesel Trucks. The carbon intensity of diesel during the vehicle's use phase is 2.627 kg of $CO_2$ equivalent per litre of diesel. The cost of greenhouse gas emissions for a fuel truck on the road is calculated at 0.5 yuan/km. Diesel costs 6.5 yuan/l, while electricity costs 1.04 yuan/kWh. This study assumes an average annual mileage of 100,000 km over the vehicle's entire life span [6], resulting in a full life cycle cost of 2.12 yuan/km for a fuel truck and 2.32 yuan/km for an electric truck.

To evaluate the robustness of ALNCO's parameter settings, a sensitivity analysis was conducted by adjusting three key parameters: max-percentages, cooling rates, and pheromone retention rate ($\rho$). These parameters directly influence the efficiency of both the local and global search processes within the ALNCO framework. The analysis was carried out on three representative large-scale instances: lc101 (clustered distribution), lr101 (random distribution), and lrc101 (mixed distribution). For each instance, the parameters were varied by ±10%, and the resulting percentage deviation in total cost was recorded. The results are presented in Figure X.

As shown in Fig. 4, the cost deviation remained consistently below 5%, demonstrating the robustness of ALNCO's parameter configuration. Among the tested instances, lr101 exhibited the highest sensitivity to variations in the cooling rate, with a maximum deviation of 4.21% when the parameter was reduced by 10%. However, the overall impact of parameter fluctuations was minimal, confirming that ALNCO maintains stable performance despite moderate variations in key parameters.

These results suggest that ALNCO demonstrates relatively stable performance across different scenarios and parameter configurations. While certain parameters, such as the cooling rate in lr101, exhibit a higher sensitivity, the overall cost deviation remains within an acceptable range. This indicates that ALNCO is capable of maintaining solution quality without extensive fine-tuning, which may enhance its applicability in practical settings where parameter calibration can be complex and time-consuming. Nevertheless, as with any heuristic-based approach, further investigations

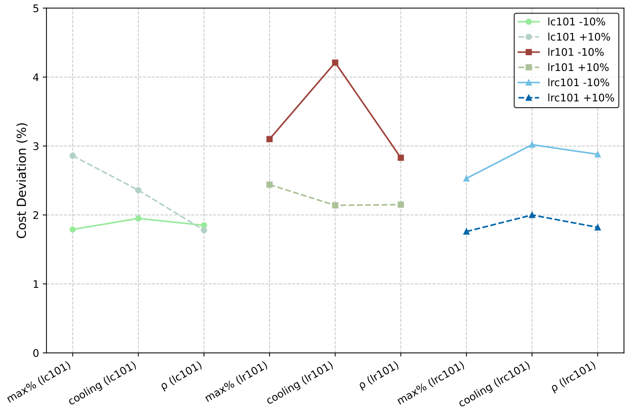

Fig. 4. Cost deviation across different parameter variations

using broader instance sets could provide deeper insights into the algorithm's adaptability across diverse operational environments.

## B. Generation Of Benchmark Examples

In order to validate the effectiveness of ALNCO, this paper uses a public dataset for experimental analyses. However, we generate new instances due to the lack of internationally recognized MDC-EFPDPTW instances based on the benchmark instances of Goeke[14] and Solomn[35]. Specifically, we combine the research results of Li[33] and refer to the current parameter configurations of fuel vans and pure electric vans Zhao[23], Amiri[25], and Li[34] to design two new sets of benchmark instances for experiments on a large instance dataset and a small instance dataset, respectively.

The large instance dataset consists of 48 instances, each containing 100 customer points. These instances are divided into three categories based on the geographical distribution of customers: random distribution (LR), cluster distribution (LC), and mixed distribution (LRC). Each type is divided into two categories based on vehicle load capacity: one for vehicles with a smaller load capacity, such as LR1, and another for vehicles with a larger load capacity, such as LR2. Next, we will describe the MDC-EFPDPTW example in detail.

To more accurately reflect the characteristics of multiple product centers in real-world scenarios, such as the varying battery capacities of different vehicles, charging demands, and the complexity of geographical layouts, we have designed new MDC-EFPDPTW instances. These instances provide a more comprehensive validation of the algorithm's applicability and address the research gap in current publicly available instances, which inadequately consider multiple product centers and the mixed substitution problem.

With the introduction of electric vehicles, the location of charging stations needed to be determined. The number of charging stations was adjusted according to the number of distribution centers based on the dataset provided by Goeke[14]. The k-means clustering method and random distribution were used to select specific charging station locations. After setting the charging stations, in order to avoid detours and time window violations caused by charging station access and charging times, and specifically to ensure that new customers do not become unreachable due to time window restrictions, a method similar to the process described in Solomn[35] was employed to generate new time windows, ensuring the feasibility of the instances.

For the configuration of the delivery points, the principle for selecting new delivery points is similar to that used for charging stations, with the locations determined using k-means clustering. Additionally, the distance between delivery points was ensured to be greater than the shortest distance from the original delivery point to the new one, thereby avoiding overlap between delivery points and achieving more balanced geographical coverage.

Regarding the setting of battery capacity, improvements were made based on the method outlined in Schneider [36]. For the LC-type instances, the battery capacity of electric vehicles was set to be sufficient to complete all delivery tasks in a 100-customer example without requiring recharging. For the LR-type instances, at least one charge is necessary to complete all tasks. Therefore, the battery capacity was set to the greater of the following two values: (1) the average distance of all LC-type instances based on the best-known solutions for the LC-type 100-customer instances in the Li and Lim instance sets, or (2) 60% of the average distance of the best-known solutions for the LR-type 100-customer instances in the Li and Lim instance sets. The specific dataset can be accessed at https://github.com/xirongfang/MDC-EFPDPTW.

## C. Mini Benchmark Example Test

*1) Example Data Description:* In the small benchmark instance, the instances are divided into two categories. In this paper, we study the hybrid vehicle path cost optimization problem, while Goeke studies the pure electric vehicle path distance optimization problem. In order to ensure that the travel time and service time in the original data remain unchanged, we improve the original dataset to form two types of instance datasets, A and B. Type A instances are the improved datasets of Goeke, which contain only one distribution center; Type B instances are improved based on the Goeke dataset, which contains two distribution centers in each dataset, to match the proposed MDC- EFPDPTW model proposed in this paper .

*2) Single Distribution Centre Instance Analysis:* For the quantitative analysis, we processed the small instance dataset using the ALNCO algorithm and compared the results with those of the commercial solver GUROBI 10.0 and Goeke's GTS algorithm, which are based on the MDC-EFPDPTW problem model presented in TABLE II.

For the Class A instance (single distribution center), TABLE II shows the algorithm's results on the small benchmark instance. In this case, $k_v$ represents the number of fuel vehicles used, $k_e$ the number of electric vehicles, $z$ the total cost, and $t$ the computation time (in seconds).The maximum computation time for the commercial solver GUROBI is set to 600 seconds, and if the optimal solution is not obtained within this time, the best feasible solution at that time is used, while for GTS and ALNCO, the average result of ten runs is used as the performance metric. In addition, Gap1 represents the percentage difference in total cost between ALNCO and GUROBI, and Gap2 represents the percentage difference in total cost between ALNCO and GTS.

In minor instances for a single distribution center, the number of instances in which ALNCO agrees with the best

TABLE II
Test results for a small benchmark example under a single distribution center

| Instance | GUROBI | | | | GTS | | | | ALNCO | | | | | |
|---|---|---|---|---|---|---|---|---|---|---|---|---|---|---|
| | $k_e$ | $k_v$ | $z$ | $t$ | $k_e$ | $k_v$ | $z$ | $t$ | $k_e$ | $k_v$ | $z$ | $t$ | Gap1 | Gap2 |
| c101c6 | 1 | 0 | 919.6 | 0.2 | 1 | 0 | 919.6 | 5.4 | 1 | 0 | 919.6 | 3.1 | 0% | 0% |
| c103c6 | 0 | 1 | 628.9 | 0.1 | 0 | 1 | 628.9 | 4.7 | 0 | 1 | 628.9 | 2.9 | 0% | 0% |
| c206c6 | 0 | 1 | 898.4 | 0.1 | 0 | 1 | 898.4 | 4.9 | 0 | 1 | 898.4 | 4.1 | 0% | 0% |
| c208c6 | 0 | 1 | 798.1 | 0.4 | 0 | 1 | 798.1 | 5.5 | 0 | 1 | 798.1 | 4.9 | 0% | 0% |
| r104c6 | 0 | 2 | 508.5 | 0.2 | 0 | 2 | 508.5 | 18.1 | 0 | 2 | 508.5 | 5.4 | 0% | 0% |
| r105c6 | 1 | 0 | 795.2 | 1.0 | 1 | 0 | 795.2 | 5.2 | 1 | 0 | 795.2 | 2.2 | 0% | 0% |
| r202c6 | 0 | 1 | 603.3 | 1.0 | 0 | 1 | 603.3 | 3.9 | 0 | 1 | 603.3 | 3.8 | 0% | 0% |
| r203c6 | 1 | 1 | 1004.7 | 1.2 | 1 | 1 | 1004.7 | 4.4 | 1 | 1 | 1004.7 | 7.2 | 0% | 0% |
| rc105c6 | 1 | 0 | 1092.3 | 1.1 | 1 | 0 | 1092.3 | 6.5 | 1 | 0 | 1092.3 | 3.7 | 0% | 0% |
| rc108c6 | 1 | 0 | 1144.1 | 0.8 | 1 | 0 | 1144.1 | 7.4 | 1 | 0 | 1144.1 | 3.3 | 0% | 0% |
| rc204c6 | 0 | 1 | 688.8 | 0.7 | 0 | 1 | 688.8 | 3.3 | 0 | 1 | 688.8 | 8.1 | 0% | 0% |
| rc208c6 | 0 | 1 | 742.3 | 0.9 | 0 | 1 | 742.3 | 5.2 | 0 | 1 | 742.3 | 8.6 | 0% | 0% |
| c104c10 | 0 | 2 | 1133.1 | 0.1 | 0 | 2 | 1133.1 | 17.8 | 0 | 2 | 1133.1 | 7.4 | 0% | 0% |
| c205c10 | 0 | 2 | 1122.0 | 0.5 | 0 | 2 | 1122.0 | 24.8 | 0 | 2 | 1122.0 | 6.0 | 0% | 0% |
| r201c10 | 0 | 1 | 887.6 | 1.2 | 0 | 1 | 887.6 | 7.3 | 0 | 1 | 887.6 | 4.6 | 0% | 0% |
| r203c10 | 1 | 0 | 1177.9 | 1.5 | 1 | 0 | 1177.9 | 6.6 | 1 | 0 | 1177.9 | 3.1 | 0% | 0% |
| rc108c10 | 1 | 1 | 1684.8 | 1.1 | 1 | 1 | 1684.8 | 37.6 | 1 | 1 | 1684.8 | 7.4 | 0% | 0% |
| rc201c10 | 0 | 2 | 1359.6 | 1.9 | 0 | 2 | 1359.6 | 8.1 | 0 | 2 | 1359.6 | 3.9 | 0% | 0% |
| rc205c10 | 1 | 1 | 1711.8 | 1.0 | 1 | 0 | 1711.8 | 22.9 | 1 | 0 | 1711.8 | 5.1 | 0% | 0% |
| c101c12 | 0 | 3 | 1175.8 | 0.8 | 0 | 3 | 1175.8 | 6.3 | 1 | 1 | 1175.8 | 3.0 | 0% | 0% |
| c202c12 | 0 | 1 | 911.1 | 1.0 | 0 | 1 | 911.1 | 6.9 | 0 | 1 | 911.1 | 2.3 | 0% | 0% |
| r102c12 | 1 | 2 | 1121.8 | 1.6 | 1 | 2 | 1121.8 | 8.7 | 1 | 2 | 1121.8 | 4.7 | 0% | 0% |
| r103c12 | 1 | 1 | 788.8 | 13.4 | 1 | 1 | 788.8 | 9.6 | 1 | 1 | 788.8 | 6.2 | 0% | 0% |
| rc102c12 | 1 | 2 | 1790.6 | 1.6 | 1 | 2 | 1790.6 | 23.4 | 1 | 2 | 1790.6 | 12.1 | 0% | 0% |
| c103c16 | 0 | 3 | 1545.6 | 2.6 | 0 | 3 | 1545.6 | 37.3 | 0 | 3 | 1545.6 | 8.0 | 0% | 0% |
| c106c16 | 0 | 3 | 1326.6 | 7.9 | 0 | 3 | 1326.6 | 46.5 | 0 | 3 | 1326.6 | 7.7 | 0% | 0% |
| c202c16 | 0 | 2 | 1664.0 | 17.2 | 0 | 2 | 1664.0 | 52.8 | 0 | 2 | 1664.0 | 7.6 | 0% | 0% |
| c208c16 | 0 | 2 | 1393.1 | 4.1 | 0 | 2 | 1393.1 | 46.4 | 0 | 2 | 1393.1 | 6.9 | 0% | 0% |
| r105c16 | 0 | 4 | 1421.4 | 3.6 | 0 | 4 | 1421.4 | 24.1 | 2 | 0 | 1449.6 | 5.7 | -2.2% | -2.2% |
| r202c16 | 1 | 1 | 1551.8 | 5.7 | 1 | 1 | 1551.8 | 65.2 | 1 | 1 | 1551.8 | 6.2 | 0% | 0% |
| r209c16 | 1 | 0 | 1870.8 | 5.9 | 1 | 0 | 1928.0 | 9.5 | 1 | 0 | 1870.8 | 6.9 | 0% | 3.1% |
| rc103c16 | 2 | 0 | 2149.3 | 42.3 | 2 | 0 | 2141.6 | 35.4 | 2 | 0 | 2141.6 | 9.3 | 0% | 0% |
| rc108c16 | 0 | 3 | 1733.4 | 62.0 | 0 | 3 | 1733.4 | 6.5 | 2 | 0 | 1744.1 | 9.2 | 0% | 0% |
| rc202c16 | 1 | 0 | 1709.0 | 19.2 | 1 | 0 | 1709.0 | 41.7 | 1 | 0 | 1709.0 | 6.4 | 0% | 0% |
| rc204c16 | 1 | 0 | 1737.6 | 49.9 | 1 | 0 | 1737.6 | 8.7 | 1 | 0 | 1737.6 | 7.2 | 0% | 0% |
| r102c18 | 0 | 5 | 1464.0 | 51.2 | 0 | 5 | 1464.0 | 10.6 | 1 | 2 | 1424.6 | 7.8 | 2.8% | 2.8% |
| AVE | 0.5 | 1.4 | 1229.3 | 8.5 | 0.5 | 1.4 | 1230.7 | 17.8 | 0.6 | 1.0 | 1229.1 | 5.9 | 0.02% | 0.1% |

GUROBI solution is 34, and the number of instances in which it agrees with GTS is 33, which suggests that the three algorithms have comparable solution quality. Regarding vehicle usage, ALNCO uses slightly fewer electric vehicles than GUROBI and GTS and slightly more fuel vehicles than GUROBI and GTS. However, the overall number of vehicles used is lower, suggesting that ALNCO has the potential to optimize vehicle allocation. In terms of solution time, the average solution time of ALNCO is only 5.9 seconds, which is significantly lower than that of GUROBI and GTS, and the performance is stable in all instances, which indicates that it can provide a feasible solution quickly, and provides a good foundation for further application to more complex problems.

*3) Dual Distribution Centre Instance Analysis:* For the Class B instances (dual distribution centers), TABLE III shows the results of testing each algorithm on small benchmark instances, with the parameters remaining consistent with TABLE III.

The results show that in terms of solution quality, ALNCO is very close to GUROBI and GTS, and in some instances, ALNCO has a slightly lower objective value. However, the difference is not significant; its cost-effectiveness is more prominent. In terms of solution time, ALNCO shows a shorter solution time in several instances, especially in c101d12 and c208d16 instances; its solution time is significantly lower than that of the other two algorithms, which shows the advantage of high efficiency. In terms of Gap metrics, the gap of ALNCO is usually tiny, indicating that its solution quality is comparable to that of other algorithms and reflects better stability and adaptability. In terms of the number of vehicles used, ALNCO has less fuel vehicle use and slightly more electric vehicle use.

However, the three algorithms' total number of vehicles used is the same, indicating that ALNCO can effectively control the vehicle allocation and provide a reasonable optimization scheme. Overall, ALNCO demonstrates good feasibility and stability in the small instance of dual distribution centers and achieves a good balance between solution efficiency and quality. Although its performance is similar to

TABLE III
Test results for a small benchmark example under a dual distribution center scenario

| Instance | GUROBI | | | | GTS | | | | ALNCO | | | | | |
|---|---|---|---|---|---|---|---|---|---|---|---|---|---|---|
| | $k_e$ | $k_v$ | $z$ | $t$ | $k_e$ | $k_v$ | $z$ | $t$ | $k_e$ | $k_v$ | $z$ | $t$ | Gap1 | Gap2 |
| c101d12 | 1 | 1 | 1032.4 | 10.8 | 1 | 1 | 1032.4 | 6.3 | 1 | 1 | 1032.4 | 1.3 | 0% | 0% |
| c202d12 | 1 | 0 | 1345.7 | 4.6 | 1 | 0 | 1345.7 | 8.1 | 1 | 0 | 1345.7 | 1.5 | 0% | 0% |
| r102d12 | 1 | 1 | 881.5 | 8.3 | 1 | 1 | 881.5 | 7.9 | 1 | 1 | 881.5 | 1.0 | 0% | 0% |
| r103d12 | 1 | 1 | 746.4 | 7.2 | 1 | 1 | 746.4 | 5.6 | 1 | 1 | 746.4 | 0.5 | 0% | 0% |
| rc102d12 | 1 | 1 | 1649.6 | 600.0 | 0 | 1 | 1623.8 | 8.7 | 0 | 1 | 1605.7 | 1.4 | 2.7% | 1.1% |
| c103d16 | 2 | 0 | 1187.5 | 600.0 | 1 | 1 | 1171.0 | 11.1 | 1 | 1 | 1171.0 | 1.3 | 1.4% | 1.4% |
| c106d16 | 0 | 2 | 1314.7 | 67.2 | 0 | 2 | 1314.7 | 9.6 | 0 | 2 | 1314.7 | 1.5 | 0% | 0% |
| c202d16 | 0 | 2 | 1624.6 | 42.3 | 0 | 2 | 1624.6 | 17.8 | 0 | 2 | 1624.6 | 1.1 | 0% | 0% |
| c208d16 | 0 | 2 | 1263.9 | 32.5 | 0 | 2 | 1263.9 | 10.4 | 0 | 2 | 1263.9 | 1.0 | 0% | 0% |
| r105d16 | 1 | 1 | 1340.1 | 10.5 | 1 | 1 | 1340.1 | 11.5 | 1 | 1 | 1340.1 | 1.6 | 0% | 0% |
| r202d16 | 0 | 2 | 1626.4 | 600.0 | 0 | 2 | 1587.2 | 38.4 | 0 | 2 | 1563.5 | 2.4 | 4.0% | 1.5% |
| r209d16 | 0 | 2 | 1562.3 | 600.0 | 0 | 2 | 1513.2 | 12.5 | 0 | 2 | 1513.2 | 1.8 | 3.2% | 0% |
| rc103d16 | 2 | 0 | 1858.9 | 48.6 | 2 | 0 | 1858.9 | 19.8 | 2 | 0 | 1858.9 | 0.7 | 0% | 0% |
| rc108d16 | 2 | 0 | 1691.3 | 52.7 | 2 | 0 | 1691.3 | 42.1 | 2 | 0 | 1691.3 | 1.9 | 0% | 0% |
| rc202d16 | 1 | 0 | 1789.7 | 600.0 | 1 | 0 | 1768.3 | 7.6 | 1 | 0 | 1768.3 | 1.3 | 1.2% | 0% |
| rc204d16 | 1 | 1 | 1790.8 | 600.0 | 1 | 1 | 1718.1 | 18.8 | 1 | 1 | 1718.1 | 0.8 | 4.2% | 4.2% |
| r102d18 | 2 | 0 | 1403.0 | 52.3 | 2 | 0 | 1403.0 | 23.8 | 2 | 0 | 1403.0 | 3.2 | 0% | 0% |
| AVE | 0.9 | 0.9 | 1418.2 | 231.6 | 0.8 | 1.0 | 1300.9 | 17.0 | 0.8 | 1.0 | 1298.5 | 1.4 | 1.0% | 0.5% |

that of GUROBI and GTS in some scenarios, ALNCO still provides short solution times and stable optimization results, which provides a solid foundation for further expansion to more complex instances.

In the small-scale dual-commodity center instance test, some instances (such as rc204d16 and rc102d12) showed obvious differences in the solutions of different algorithms. This difference is mainly due to the increased differences in the layout of commodity centers. The customer demand distribution of the rc204d16 instance is more dispersed, and the commodity window is tighter, resulting in a more complex solution space. The Gurobi, GTS, and ALNCO solution methods may differ in the excitation process due to different exploration paths. In addition, the adaptive and perturbation mechanism of the ALNCO algorithm can more effectively support local optimality, thereby obtaining a flatter and more stable solution.

*4) Comparison Of Differences In Different Solution Instances And Computing Time Of Same Solution Instances:* Combining the results in TABLES II and III, we find that most instances have the same final solution under the three algorithms under a single distribution center. In contrast, the number of instances with different solutions increases significantly under a dual distribution center. For these instances with different solutions, we extract the optimal solution of each algorithm and further analyze the difference (see TABLE IV).

TABLE IV
Comparison of solution differences between algorithms

| Comparison | Number of Differences/Total | Maximum Difference | Average Difference |
|---|---|---|---|
| GTS vs Gurobi | 8/53 | 4.2% | 3.3% |
| ALNCO vs Gurobi | 7/53 | 4.2% | 2.2% |

The results show that the number of differences between GTS and GUROBI, as well as ALNCO and GUROBI, is not very different; however, in terms of the maximum difference, the maximum difference of 4.2% occurs for both GTS and ALNCO, and both of them are found in rc204d16 instances under dual distribution centers. Regarding the average value of the differences, ALNCO slightly outperforms GTS, which indicates that in most instances, ALNCO can maintain a slight cost difference, reflecting its stability and reliability in dealing with problems with different distribution centers.

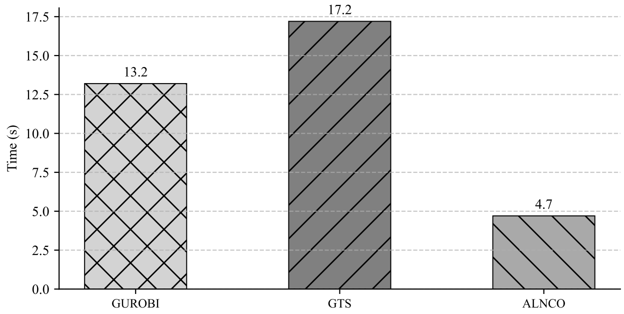

Fig. 5. Computation time comparison

In addition, when comparing the computation times of the same optimal solution instances (shown in Fig. 5), it can be seen that although none of GUROBI's computation times reaches the set maximum computation time, ALNCO's average computation time is the shortest, significantly better than that of GUROBI and GTS, further proving its superiority in terms of computational efficiency.

### *D. Large-scale Benchmarking Example Test*

In order to address the problem of significant instances of the MDC-EFPDPTW model, this study improves the ALNS algorithm proposed by Wang et al.[10] and the GTS algorithm by Goeke[14] to better suit the specific needs of the model. The study compares the performance of the three algorithms by evaluating them in terms of cost, number of vehicles used, and running time. Further, the stability of the ALNCO algorithm proposed in this paper is assessed by analyzing the convergence curves of different types of instances.

*1) Algorithm Performance Comparison:* As shown in TABLE V, this study systematically compares the performance of the three algorithms, GTS, ALNS, and ALNCO, on large benchmark instances. It focuses on evaluating their cost performance in multi-distribution center path optimization.

Specifically, ALNCO demonstrates significant advantages in three key metrics: minimum cost, average cost, and standard deviation. By comparison, ALNCO outperforms in minimum cost, with a 10.6% reduction compared to GTS and a 14.2% reduction compared to ALNS. This result shows that ALNCO has a significant advantage in cost optimization and can reduce transport costs effectively. Regarding average cost, ALNCO outperforms GTS and ALNS with a reduction of 12.5 %and 16.7 %, respectively, reflecting strong adaptability and stability. ALNCO also outperforms the standard deviation, with a 31 percent reduction compared to GTS and a 45.1 percent reduction compared to ALNS. This suggests that ALNCO can provide more consistent and reliable solutions, reducing the occurrence of extreme solutions and enhancing the stability of optimization results. ALNCO performs well in several key indicators, especially regarding stability and adaptability, showing its strong practicality and operability in the multi-distribution center path optimization problem.

*2) Vehicle Allocation Optimization And Operational Efficiency Analysis:* As shown in TABLE VI, in order to further evaluate the performance of the algorithms, this study also compares the performance of the three algorithms, GTS, ALNS, and ALNCO, by analyzing the four core metrics, namely, the total number of vehicles $K$, the number of trolley use $k_e$, the number of fuel vehicle use $k_v$, and the running time $t$. The results show that ALNCO has significant advantages in vehicle allocation optimization and improving operational efficiency, especially in reducing fleet size and optimizing vehicle usage structure.

Specifically, the average total vehicle size of ALNCO is 6.3, which is lower than that of GTS (7.5) and ALNS (9.1), indicating that ALNCO can effectively reduce vehicle inputs, optimize resource allocation, and reduce costs. In terms of vehicle use, ALNCO improves system efficiency by reducing the use of fuel vehicles and increasing the proportion of trams. The experimental data show that the number of fuel vehicles ALNCO uses in most instances is significantly lower than that of GTS and ALNS, and the proportion of trams used is higher, especially in the scenarios where EVs are more applicable. The average number of trams used by ALNCO is 3.1, higher than that of ALNS (2.6) but slightly lower than that of GTS (3.4). In comparison, the number of fuel vehicles used is 3.2, significantly lower than that of GTS (4.1) and 6.4 for ALNS, further validating its advantages. Regarding running time, ALNCO also shows a significant advantage in computational efficiency, especially in path optimization and vehicle scheduling, which can effectively shorten the computation time. The experimental data show that the computation time of ALNCO is significantly lower than that of ALNS in most instances, and the gap with GTS is smaller. The average running time of ALNCO is 234.5 seconds, which is slightly higher than that of GTS (227.6 seconds) but significantly lower than that of ALNS (361.2 seconds), demonstrating its good balance between computational efficiency and quality.

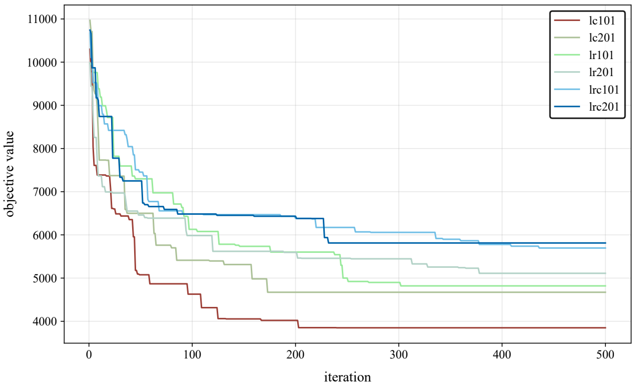

Fig. 6. Convergence curves of different instances of the ALNCO

Furthermore, to more clearly illustrate the differences in the usage ratios of electric and fuel vehicles under various algorithms, we further examined the comparative vehicle configuration ratios, as shown in TABLE VII. As evident from the figure, the ALNCO algorithm tends to favor a higher proportion of electric vehicles, thereby offering significant advantages in terms of reducing overall costs and carbon emissions.

*3) Convergence Analysis And Stability Assessment:* In this section, we choose LC101, LC201, LR101, LR201, LRC101, and LRC201 as examples to analyze the convergence of the proposed algorithm.

Fig. 6 demonstrates the trend of the objective function value as the number of iterations increases. The figure shows that the ALNCO algorithm converges faster, especially in the LC101 and LR101 instances, where the objective function value decreases rapidly, indicating the algorithm has a strong global search capability. This suggests that the algorithm can quickly reduce the solution space in these instances and find a better initial solution. As the number of iterations increases, the convergence curves for all instances gradually flatten out, indicating that the algorithm is starting to shift to local search and fine-tune the solution. Eventually, the convergence curves of all instances stabilize, indicating that the ALNCO algorithm has successfully converged to a stable solution. Although the convergence speed varies from instance to instance, ALNCO consistently shows good optimization performance, reflecting the adaptability of the algorithm in a wide range of situations.

Overall, the ALNCO algorithm exhibits desirable convergence when dealing with the MDC-EFPDPTW problem and can find a high-quality solution within a small number of iterations with good stability.

## VI. Conclusion

This paper addresses a novel vehicle routing problem: the mixed fuel and electric vehicle delivery route optimization problem within a multi-distribution centre context. The objective is to minimize total costs while analyzing the impact of fuel and electric vehicle selection in various transport scenarios. This analysis provides empirical insights and

TABLE V
Multi-distribution center cost comparison on large benchmark instances

| Instance | GTS | | | ALNS | | | ALNCO | | |
|---|---|---|---|---|---|---|---|---|---|
| | Best | Avg | Std | Best | Avg | Std | Best | Avg | Std |
| lc101 | 4672.0 | 5026.8 | 64.1 | 4820.2 | 5236.8 | 80.3 | 3863.2 | 4057.4 | 40.4 |
| lc102 | 4715.7 | 4982.5 | 48.1 | 4869.1 | 5195.7 | 63.9 | 3997.8 | 4123.3 | 37.9 |
| lc103 | 5025.6 | 5429.2 | 72.9 | 5178.3 | 5644.6 | 89.3 | 4120.7 | 4352.8 | 47.3 |
| lc104 | 4911.2 | 5345.6 | 78.5 | 5025.6 | 5521.1 | 94.6 | 4198.7 | 4368.3 | 54.1 |
| lc105 | 3862.0 | 4429.3 | 102.7 | 4090.1 | 4737.0 | 122.2 | 3302.6 | 3684.9 | 74.6 |
| lc106 | 4787.1 | 5192.7 | 73.3 | 4781.9 | 5240.2 | 87.9 | 3991.7 | 4229.9 | 48.4 |
| lc107 | 4191.4 | 4524.2 | 60.1 | 4257.7 | 4647.7 | 75.5 | 3616.4 | 3801.3 | 38.7 |
| lc108 | 4917.3 | 5294.0 | 68.1 | 5002.6 | 5437.5 | 83.7 | 4133.3 | 4349.5 | 44.4 |
| lc201 | 5300.3 | 5788.6 | 88.3 | 5922.4 | 6510.6 | 111.4 | 4672.0 | 4798.2 | 64.4 |
| lc202 | 6844.1 | 7238.0 | 71.2 | 6931.4 | 7382.9 | 86.7 | 5426.6 | 5642.8 | 44.4 |
| lc203 | 6639.2 | 7065.9 | 77.1 | 6950.2 | 7446.3 | 94.7 | 5617.4 | 5677.6 | 52.4 |
| lc204 | 6244.5 | 6555.6 | 56.1 | 6226.5 | 6590.8 | 70.7 | 4953.8 | 5104.6 | 32.5 |
| lc205 | 6257.0 | 6794.5 | 97.2 | 6499.3 | 7107.1 | 115.0 | 5477.9 | 5744.8 | 71.8 |
| lc206 | 5387.5 | 5880.4 | 89.1 | 5519.9 | 6075.5 | 105.6 | 4651.8 | 4974.7 | 63.8 |
| lc207 | 6648.6 | 7056.9 | 73.8 | 6738.3 | 7204.5 | 89.3 | 5490.4 | 5728.6 | 48.4 |
| lc208 | 7122.8 | 7479.7 | 64.4 | 7310.4 | 7728.3 | 80.5 | 5678.4 | 5866.5 | 39.3 |
| lr101 | 5063.9 | 5462.7 | 72.1 | 5161.0 | 5619.0 | 87.8 | 4819.4 | 5089.0 | 54.1 |
| lr102 | 5499.3 | 5769.9 | 48.7 | 5565.0 | 5891.8 | 64.0 | 5217.6 | 5365.1 | 31.9 |
| lr103 | 5534.5 | 5866.8 | 60.0 | 5690.7 | 6083.6 | 76.0 | 5485.7 | 5701.9 | 44.4 |
| lr104 | 5533.8 | 5839.7 | 55.2 | 5512.5 | 5871.3 | 69.8 | 5116.5 | 5292.0 | 37.0 |
| lr105 | 5353.8 | 5782.5 | 77.4 | 5398.3 | 5883.0 | 92.6 | 4900.6 | 5186.1 | 57.0 |
| lr106 | 5332.3 | 5584.0 | 45.4 | 5423.5 | 5732.1 | 60.7 | 5119.0 | 5250.5 | 29.0 |
| lr107 | 4978.6 | 5358.4 | 68.6 | 5041.5 | 5478.3 | 83.9 | 4727.8 | 4978.7 | 50.7 |
| lr108 | 5464.6 | 5808.1 | 62.0 | 5690.5 | 6098.3 | 78.7 | 5051.9 | 5262.0 | 43.3 |
| lr201 | 5523.1 | 5774.5 | 45.3 | 5693.4 | 6004.0 | 61.0 | 5111.0 | 5236.5 | 27.9 |
| lr202 | 6519.1 | 6866.5 | 62.7 | 6688.0 | 7096.0 | 78.7 | 5619.3 | 5816.8 | 41.0 |
| lr203 | 5776.1 | 6135.1 | 64.9 | 6092.0 | 6519.5 | 82.3 | 5362.5 | 5588.1 | 46.1 |
| lr204 | 6206.8 | 6509.2 | 54.5 | 6630.5 | 7001.6 | 72.0 | 5561.8 | 5728.0 | 35.3 |
| lr205 | 5977.4 | 6274.2 | 53.5 | 6730.2 | 7107.6 | 73.2 | 5761.2 | 5936.7 | 37.0 |
| lr206 | 6489.3 | 6754.8 | 47.8 | 6445.0 | 6763.4 | 62.5 | 5533.4 | 5658.8 | 27.9 |
| lr207 | 6028.8 | 6488.6 | 83.1 | 6720.5 | 7276.3 | 105.5 | 5716.2 | 6042.4 | 64.4 |
| lr208 | 5975.2 | 6373.8 | 72.0 | 6175.0 | 6637.4 | 88.6 | 5510.1 | 5770.3 | 52.4 |
| lrc101 | 5936.3 | 6521.2 | 105.8 | 6395.4 | 7071.3 | 127.4 | 5563.7 | 6002.7 | 84.9 |
| lrc102 | 6309.0 | 6805.4 | 89.8 | 6404.6 | 6960.2 | 105.6 | 5830.4 | 6181.3 | 68.9 |
| lrc103 | 5838.0 | 6276.2 | 79.2 | 6087.4 | 6593.9 | 96.6 | 5144.5 | 5426.7 | 56.4 |
| lrc104 | 5412.0 | 5747.6 | 60.6 | 5670.0 | 6071.1 | 77.5 | 5091.7 | 5298.6 | 42.7 |
| lrc105 | 6031.0 | 6319.1 | 52.0 | 6422.1 | 6777.3 | 69.2 | 5685.8 | 5848.7 | 34.7 |
| lrc106 | 7231.6 | 7637.1 | 73.3 | 7146.9 | 7602.4 | 87.4 | 5947.4 | 6182.3 | 47.8 |
| lrc107 | 6635.2 | 6908.3 | 49.2 | 6983.1 | 7320.2 | 65.8 | 6208.6 | 6356.1 | 31.9 |
| lrc108 | 6550.7 | 6855.2 | 55.0 | 6865.3 | 7234.3 | 71.7 | 5713.3 | 5876.2 | 34.7 |
| lrc201 | 6000.7 | 6257.2 | 46.2 | 6260.8 | 6578.9 | 62.4 | 5831.3 | 5969.4 | 30.2 |
| lrc202 | 7021.5 | 7392.1 | 66.9 | 7601.6 | 8049.4 | 86.0 | 6333.7 | 6562.6 | 46.7 |
| lrc203 | 6449.4 | 6794.6 | 62.3 | 6959.2 | 7378.7 | 80.8 | 5840.9 | 6047.8 | 42.7 |
| lrc204 | 5547.4 | 5878.6 | 59.8 | 6041.4 | 6448.1 | 78.5 | 5235.8 | 5439.4 | 42.1 |
| lrc205 | 6796.9 | 7061.9 | 47.8 | 7267.9 | 7599.6 | 64.9 | 6162.9 | 6297.7 | 29.6 |
| lrc206 | 6932.7 | 7290.7 | 64.6 | 7744.5 | 8188.2 | 85.2 | 6541.1 | 6680.0 | 46.7 |
| lrc207 | 7052.3 | 7369.7 | 57.3 | 7356.5 | 7738.0 | 73.9 | 6475.9 | 6660.8 | 38.7 |
| lrc208 | 5967.1 | 6247.1 | 50.4 | 6402.9 | 6751.2 | 67.8 | 5487.6 | 5638.4 | 32.5 |
| AVG | 5843.6 | 6210.3 | 66.2 | 6091.5 | 6523.6 | 83.1 | 5227.1 | 5434.9 | 45.7 |

TABLE VI
MULTI-DISTRIBUTION CENTER VEHICLE USAGE AND EFFICIENCY COMPARISON ON LARGE BENCHMARK INSTANCES

| Instance | GTS | | | | ALNS | | | | ALNCO | | | |
|---|---|---|---|---|---|---|---|---|---|---|---|---|
| | $k_e$ | $k_v$ | $z$ | $t$ | $k_e$ | $k_v$ | $z$ | $t$ | $k_e$ | $k_v$ | $z$ | $t$ |
| lc101 | 5 | 5 | 10 | 62.9 | 4 | 8 | 12 | 321.5 | 6 | 4 | 10 | 103.5 |
| lc102 | 4 | 7 | 11 | 68.5 | 4 | 8 | 12 | 517.9 | 7 | 3 | 10 | 134.8 |
| lc103 | 5 | 6 | 11 | 331.9 | 5 | 8 | 13 | 488.1 | 7 | 4 | 11 | 242.9 |
| lc104 | 6 | 5 | 11 | 404.9 | 5 | 7 | 12 | 376.5 | 7 | 4 | 11 | 166.5 |
| lc105 | 7 | 4 | 11 | 190.1 | 5 | 6 | 11 | 606.8 | 7 | 3 | 10 | 578.1 |
| lc106 | 3 | 8 | 11 | 156.5 | 2 | 11 | 13 | 497.3 | 7 | 3 | 10 | 408.6 |
| lc107 | 4 | 7 | 11 | 249.1 | 4 | 8 | 12 | 237.9 | 5 | 4 | 9 | 257.1 |
| lc108 | 6 | 5 | 11 | 242.7 | 5 | 5 | 10 | 266.3 | 6 | 4 | 10 | 241.6 |
| lc201 | 2 | 1 | 3 | 320.9 | 2 | 5 | 7 | 538.6 | 3 | 1 | 4 | 352.0 |
| lc202 | 2 | 2 | 4 | 91.5 | 0 | 6 | 6 | 310.4 | 1 | 3 | 4 | 165.2 |
| lc203 | 1 | 3 | 4 | 124.8 | 0 | 5 | 5 | 146.3 | 2 | 2 | 4 | 72.6 |
| lc204 | 3 | 2 | 5 | 66.5 | 3 | 3 | 6 | 103.4 | 4 | 1 | 5 | 83.3 |
| lc205 | 1 | 3 | 4 | 86.0 | 3 | 3 | 6 | 177.4 | 1 | 3 | 4 | 127.9 |
| lc206 | 3 | 1 | 4 | 46.9 | 1 | 4 | 5 | 392.3 | 4 | 1 | 5 | 97.4 |
| lc207 | 3 | 1 | 4 | 43.2 | 2 | 3 | 5 | 163.2 | 3 | 2 | 5 | 83.1 |
| lc208 | 2 | 2 | 4 | 88.5 | 2 | 6 | 8 | 146.5 | 2 | 2 | 4 | 101.7 |
| lr101 | 8 | 6 | 14 | 34.5 | 6 | 7 | 13 | 242.3 | 6 | 5 | 11 | 53.6 |
| lr102 | 5 | 10 | 15 | 45.3 | 4 | 13 | 17 | 311.5 | 3 | 5 | 8 | 48.5 |
| lr103 | 5 | 9 | 14 | 76.7 | 4 | 9 | 13 | 255.9 | 3 | 5 | 8 | 214.4 |
| lr104 | 4 | 9 | 13 | 449.0 | 4 | 11 | 15 | 536.0 | 4 | 5 | 9 | 562.3 |
| lr105 | 5 | 6 | 11 | 358.7 | 3 | 10 | 13 | 477.0 | 3 | 5 | 8 | 303.9 |
| lr106 | 5 | 3 | 8 | 99.6 | 4 | 6 | 10 | 175.3 | 5 | 2 | 7 | 192.5 |
| lr107 | 4 | 3 | 7 | 795.6 | 2 | 5 | 7 | 907.1 | 4 | 3 | 7 | 283.8 |
| lr108 | 3 | 5 | 8 | 259.3 | 3 | 9 | 12 | 329.4 | 3 | 4 | 7 | 319.2 |
| lr201 | 4 | 2 | 6 | 53.7 | 3 | 2 | 5 | 327.5 | 2 | 3 | 5 | 152.1 |
| lr202 | 2 | 2 | 4 | 109.2 | 1 | 5 | 6 | 188.9 | 1 | 2 | 3 | 168.5 |
| lr203 | 2 | 2 | 4 | 908.9 | 2 | 4 | 6 | 536.9 | 1 | 2 | 3 | 311.4 |
| lr204 | 1 | 2 | 3 | 121.3 | 0 | 5 | 5 | 342.3 | 1 | 2 | 3 | 301.5 |
| lr205 | 1 | 2 | 3 | 106.7 | 0 | 5 | 5 | 181.1 | 1 | 2 | 3 | 134.8 |
| lc206 | 1 | 2 | 3 | 166.3 | 1 | 3 | 4 | 249.2 | 0 | 3 | 3 | 205.7 |
| lc207 | 1 | 3 | 4 | 175.2 | 0 | 5 | 5 | 228.8 | 1 | 3 | 4 | 233.0 |
| lc208 | 3 | 2 | 5 | 186.0 | 2 | 4 | 6 | 246.3 | 3 | 2 | 5 | 125.8 |
| lrc101 | 6 | 7 | 13 | 296.0 | 4 | 11 | 15 | 327.4 | 3 | 4 | 7 | 215.6 |
| lrc102 | 5 | 6 | 11 | 434.7 | 4 | 9 | 13 | 742.2 | 5 | 4 | 9 | 459.6 |
| lrc103 | 4 | 8 | 12 | 845.6 | 4 | 10 | 14 | 796.0 | 4 | 5 | 9 | 505.3 |
| lrc104 | 7 | 6 | 13 | 275.0 | 5 | 9 | 14 | 590.4 | 3 | 3 | 6 | 373.7 |
| lrc105 | 3 | 5 | 8 | 559.0 | 1 | 7 | 8 | 461.6 | 3 | 4 | 7 | 364.1 |
| lrc106 | 5 | 3 | 8 | 351.5 | 5 | 5 | 10 | 547.1 | 6 | 3 | 9 | 430.1 |
| lrc107 | 5 | 5 | 10 | 426.4 | 4 | 9 | 13 | 494.4 | 4 | 5 | 9 | 371.1 |
| lrc108 | 6 | 5 | 11 | 20.6 | 5 | 6 | 11 | 414.1 | 3 | 4 | 7 | 77.3 |
| lrc201 | 1 | 3 | 4 | 88.5 | 2 | 5 | 7 | 346.5 | 1 | 3 | 4 | 78.1 |
| lrc202 | 1 | 3 | 4 | 131.2 | 1 | 6 | 7 | 206.2 | 1 | 3 | 4 | 176.6 |
| lrc203 | 1 | 3 | 4 | 187.2 | 1 | 6 | 7 | 248.6 | 0 | 3 | 3 | 273.2 |
| lrc204 | 2 | 3 | 5 | 85.4 | 2 | 7 | 9 | 209.6 | 1 | 2 | 3 | 173.5 |
| lrc205 | 1 | 4 | 5 | 116.7 | 0 | 5 | 5 | 210.7 | 1 | 4 | 5 | 246.4 |
| lrc206 | 2 | 2 | 4 | 144.5 | 1 | 5 | 6 | 346.7 | 1 | 3 | 4 | 330.4 |
| lrc207 | 1 | 3 | 4 | 195.3 | 1 | 5 | 6 | 199.6 | 0 | 3 | 3 | 111.8 |
| lrc208 | 1 | 3 | 4 | 247.0 | 1 | 4 | 5 | 369.7 | 0 | 3 | 3 | 239.9 |
| AVE | 3.4 | 4.1 | 7.5 | 227.6 | 2.6 | 6.4 | 9.1 | 361.2 | 3.1 | 3.2 | 6.3 | 234.5 |

Table VII
VEHICLE CONFIGURATION RATIO OF ALGORITHMS GTS, ALNS AND ALNCO

| Algorithm | Electric Vehicle | Fuel Vehicle |
|---|---|---|
| GTS | 4801.23 | 868.8956 |
| ALNS | 4683.74 | 1241.245 |
| ALNCO | 4671.42 | 1473.584 |

strategic recommendations for these vehicle types' future application and development. Particular emphasis is placed on charging-related issues, such as battery capacity constraints, the possibility of en-route charging, and the relationship between charging time and volume, to capture the complexity of real-world transport operations better. Additionally, the environmental impact of fuel trucks is incorporated through introducing carbon emission costs, offering a new comparative dimension when choosing between pure electric and fuel-powered trucks.By developing a hybrid ALNCO heuristic algorithm, this study demonstrates the efficiency and practical value of the proposed method on a newly designed MDC-EFPDPTW benchmark. The results provide algorithmic solid support for routing and charging decisions in real-world transport operations and encourage the adoption and profitable utilization of electric trucks in the transport market, thereby promoting green logistics practices. Future research will explore more comprehensive vehicle procurement cost models and optimize charging station locations and density further to enhance the development of green and efficient transportation modes.

## REFERENCES

[1] Chen Ping,"Development of highway logistics in China," Contemporary Logistics in China: Collaboration and Reciprocation, pp95-114, 2018

[2] Chen Heng, and Yan Zhang, "Research on the path of sustainable development of China’s logistics industry driven by capital factors," Sustainability, vol. 15, no. 1, pp297, 2022

[3] Desaulniers, Guy, et al., "VRP with Pickup and Delivery," The Vehicle Routing Problem, vol. 9, pp225-242, 2002

[4] Ropke, Stefan, and David Pisinger. "An adaptive large neighborhood search heuristic for the pickup and delivery problem with time windows." Transportation science 40.4 (2006): 455-472.

[5] Weldon, Peter, Patrick Morrissey, and Margaret O’Mahony, "Long-term cost of ownership comparative analysis between electric vehicles and internal combustion engine vehicles," Sustainable Cities and Society, vol. 39, pp578-591, 2018

[6] Mao, Shiyue, et al., "Total Cost of Ownership for Heavy Trucks in China: Battery Electric, Fuel Cell Electric and Diesel Trucks," White Paper, International Council on Clean Transportation, 2021.

[7] Aguilar, P., and Bodo Groß, "Battery electric vehicles and fuel cell electric vehicles, an analysis of alternative powertrains as a mean to decarbonise the transport sector," Sustainable Energy Technologies and Assessments, vol. 53, pp102624, 2022.

[8] Kucukoglu, Ilker, Reginald Dewil, and Dirk Cattrysse, "The electric vehicle routing problem and its variations: A literature review," Computers & Industrial Engineering, vol. 161, pp107650, 2021.

[9] Bogyrbayeva, Aigerim, et al., "Learning to solve vehicle routing problems: A survey," arXiv preprint arXiv:2205.02453, 2022.

[10] Wang, Xin, Herbert Kopfer, and Michel Gendreau, "Operational transportation planning of freight forwarding companies in horizontal coalitions," European Journal of Operational Research, vol. 237, no. 3, pp1133-1141, 2014.

[11] Louati, Ali, et al., "Mixed integer linear programming models to solve a real-life vehicle routing problem with pickup and delivery," Applied Sciences, vol. 11, no. 20, pp9551, 2021.

[12] Polat, Olcay, et al., "A perturbation based variable neighborhood search heuristic for solving the vehicle routing problem with simultaneous pickup and delivery with time limit," European Journal of Operational Research, vol. 242, no. 2, pp369-382, 2015.

[13] Wang, Chao, et al., "A parallel simulated annealing method for the vehicle routing problem with simultaneous pickup–delivery and time windows," Computers & Industrial Engineering, vol. 83, pp111-122, 2015.

[14] Goeke, Dominik, "Granular tabu search for the pickup and delivery problem with time windows and electric vehicles," European Journal of Operational Research, vol. 278, no. 3, pp821-836, 2019.

[15] Zhang, Huizhen, et al., "A hybrid ant colony optimization algorithm for a multi-objective vehicle routing problem with flexible time windows," Information Sciences, vol. 490, pp166-190, 2019.

[16] Phuc, Phan Nguyen Ky, and Nguyen Le Phuong Thao, "Ant colony optimization for multiple pickup and multiple delivery vehicle routing problem with time window and heterogeneous fleets," Logistics, vol. 5, no. 2, pp1-13, 2021.

[17] Keçeci, Bariş, Fulya Altıparmak, and İmdat Kara, "A mathematical formulation and heuristic approach for the heterogeneous fixed fleet vehicle routing problem with simultaneous pickup and delivery," Journal of Industrial and Management Optimization, vol. 17, no. 3, pp1069-1100, 2021.

[18] Kumar, Ritesh, Nikhil Kori, and Vijay Kumar Chaurasiya, "Real-time data sharing, path planning and route optimization in urban traffic management," Multimedia Tools and Applications, vol. 82, no. 23, pp36343-36361, 2023.

[19] Wu, Qichao, et al., "A neighborhood comprehensive learning particle swarm optimization for the vehicle routing problem with time windows," Swarm and Evolutionary Computation, vol. 84, pp101425, 2024.

[20] Sassi, Ons, Wahiba Ramdane Cherif, and Ammar Oulamara, "Vehicle routing problem with mixed fleet of conventional and heterogeneous electric vehicles and time dependent charging costs," 2014.

[21] Ying, L. I., Z. H. A. N. G. Pengwei, and W. U. Yifan, "Vehicle routing problem with mixed fleet of conventional and electric vehicles," Journal of Systems & Management, vol. 29, no. 3, pp522, 2020.

[22] Hatami, Sara, et al., "Green hybrid fleets using electric vehicles: solving the heterogeneous vehicle routing problem with multiple driving ranges and loading capacities," SORT: Statistics and Operations Research Transactions, vol. 44, no. 1, 2020.

[23] Zhao, Peixin, et al., "Bi‐Objective Optimization for Vehicle Routing Problems with a Mixed Fleet of Conventional and Electric Vehicles and Soft Time Windows," Journal of Advanced Transportation, vol. 2021, no. 1, pp9086229, 2021.

[24] Celebi, Dilay, "Planning a mixed fleet of electric and conventional vehicles for urban freight with routing and replacement considerations," Sustainable Cities and Society, vol. 73, pp103105, 2021.

[25] Amiri, Afsane, Saman Hassanzadeh Amin, and Hossein Zolfagharinia, "A bi-objective green vehicle routing problem with a mixed fleet of conventional and electric trucks: Considering charging power and density of stations," Expert Systems with Applications, vol. 213, pp119228, 2023.

[26] Shi, Yanjun, et al., "A method for transportation planning and profit sharing in collaborative multi-carrier vehicle routing," Mathematics, vol. 8, no. 10, pp1788, 2020.

[27] Anuar, Wadi Khalid, et al., "A multi-depot dynamic vehicle routing problem with stochastic road capacity: An MDP model and dynamic policy for post-decision state rollout algorithm in reinforcement learning," Mathematics, vol. 10, no. 15, pp2699, 2022.

[28] Zhang, Jian, et al., "Solving large-scale dynamic vehicle routing problems with stochastic requests," European Journal of Operational Research, vol. 306, no. 2, pp596-614, 2023.

[29] Yan-e Hou, Lanxue Dang, Hengrui Ma, and Chunyang Zhang, "A Selection Hyper-heuristic for the Multi-compartment Vehicle Routing Problem Considering Carbon Emission," Engineering Letters, vol. 32, no. 10, pp2002-2011, 2024

[30] Chunxiao Wang, Hengrui Ma, Defeng Zhu, and Yan-e Hou, "A Hybrid Genetic Algorithm for Multi-compartment Open Vehicle Routing Problem with Time Window in Fresh Products Distribution," Engineering Letters, vol. 32, no. 6, pp1201-1209, 2024

[31] Kabadurmus, Ozgur, and Mehmet S. Erdogan, "A green vehicle routing problem with multi-depot, multi-tour, heterogeneous fleet

and split deliveries: a mathematical model and heuristic approach," Journal of Combinatorial Optimization, vol. 45, no. 3, pp89, 2023.

[32] Ma, Lingji, and Meiyan Li, "Research on a Joint Distribution Vehicle Routing Problem Considering Simultaneous Pick-Up and Delivery under the Background of Carbon Trading," Sustainability, vol. 16, no. 4, pp1698, 2024.

[33] Li, Haibing, and Andrew Lim, "A metaheuristic for the pickup and delivery problem with time windows," Proceedings of the 13th IEEE International Conference on Tools with Artificial Intelligence (ICTAI 2001), IEEE, pp160-167, 2001.

[34] Li, Junjie, et al., "Life cycle cost of conventional, battery electric, and fuel cell electric vehicles considering traffic and environmental policies in China," International Journal of Hydrogen Energy, vol. 46, no. 14, pp9553-9566, 2021.

[35] Solomon, Marius M., "Algorithms for the vehicle routing and scheduling problems with time window constraints," Operations Research, vol. 35, no. 2, pp254-265, 1987.

[36] Schneider, Michael, Andreas Stenger, and Dominik Goeke, "The electric vehicle-routing problem with time windows and recharging stations," Transportation Science, vol. 48, no. 4, pp500-520, 2014.